Mechanisms for Scaffold-Mediated Regulation of Kinase Activity in the Wnt Signaling Pathway

Erin Fagnan

A dissertation

submitted in partial fulfillment of the

requirements for the degree of

Doctor of Philosophy

University of Washington

2019

Reading Committee:

Jesse Zalatan, Chair

Dustin Maly

Stefan Stoll

Program Authorized to Offer Degree:

Chemistry

University of Washington

Abstract

Mechanisms for Scaffold-Mediated Regulation of Kinase Activity in the Wnt Signaling Pathway

Erin Fagnan

Chair of the Supervisory Committee:
Assistant Professor Jesse Zalatan
Department of Chemistry

Cellular signaling is a complex process involving numerous pathways. Many of these pathways are connected through shared proteins, creating branch points that may result in crosstalk between pathways. It is not fully understood how protein activity can be regulated by a variety of different upstream signals and still maintain specificity. Scaffold proteins may act as a solution to this specificity issue by physically assembling signaling proteins within a specific pathway, such as a MAPK cascade. There are many models for how scaffold proteins regulate protein activity, all of which are based on the idea that scaffold proteins increase specificity by increasing reaction rates for the proteins they bring together. Even though this idea has laid the foundation for many studies in the signaling field, we still lack a thorough kinetic analysis of scaffold function and its effect on specificity. In order to determine if scaffold proteins actually increase reaction rates as a mechanism for specificity, we measured GSK3β reaction rates with several substrates in a

minimal, biochemically reconstituted system of the Wnt signaling network. We found that the Wnt scaffold Axin produces a modest, 2-fold enhancement of the rate of phosphorylation of the Wnt substrate β-catenin. Surprisingly, we found that Axin significantly slows the rate of phosphorylation of a non-Wnt substrate. Together, these data suggest that Axin alone is not sufficient to accelerate a specific kinase-substrate reaction. Instead, Axin can promote signaling specificity by suppressing kinase reactions with competing, non-Wnt pathway targets. Further, these newly identified properties of Axin reinforce an emerging trend that scaffold proteins can regulate kinase activity through a diverse set of mechanisms.

TABLE OF CONTENTS

LIST OF ABBREVIATIONS

AKAP	A-kinase-anchoring protein
APC	Adenomatous polyposis coli
ATP	adenosine triphosphosphate
BCD	B-catenin binding domain
cAMP	Cyclic sdenosine monophosphate
CKIa	Casein Kinase I alpha
CREB	cAMP response element-binding protein
DTT	dithiothreitol
Dvl	Dishevelled
ERK	Extracellular signal-regulated Kinase
FRAT	Frequently rearranged in advanced T-cell lymphomas
Fz	Frizzled
GBP	GSK3-binding protein
GSK3B	Glycogen synthase kinase 3 beta
HEPES	4-(2-hydroyethyl)-1-piperazineethanesulfonic acid
His	Histidine
IGEPAL	octylphenoxy poly(ethyleneoxy)ethanol, branched
INAD	Inactivation-no-after-potential D
IPTG	isopropyl B-D-1-thiogalactopyranoside
JIP-1	JNK-interacting protein 1
JNK	C-Jun N-terminal Kinase
KSR	Kinase Suppressor of Ras
LAT	Linker for Activation of T-cell
LRP	Lipoprotein receptor-related protein
MAPK	Mitogen-activated protein kinase
MAPKK	Mitogen-activated protein kinase kinase
MAPKKK	Mitogen-activated protein kinase kinase kinase
MBP	Maltose binding protein
PI3K	Phosphoinositide 3-kinase
PKA	Protein kinase A
PMP	Protein MetalloPhosphatase buffer
PORCN	Porcupine o-acyltransferase
PP1	Protein Phosphatase 1
Ser	Serine
TBST	Tris-buffered saline with Tween-20
Tyr	Tyrosine

Kinetic Parameters

*k*a	rate of Association
k_{cat}	turnover number
k_{cat}/K_M	bimolecular rate constant
kd	rate of dissociation
K_D	Binding constant
K_M	substrate concentration at 1/2 Vmax

Units

C	celcius
Ci	Curie
°	degree
hr	hour
L	liter
M	molar
m	meter
min	minute
s	second

Prefixes

n	nano
u	micro
m	milli

LIST OF FIGURES

LIST OF TABLES

ACKNOWLEDGEMENTS

First and foremost, I would like to thank my advisor, Jesse Zalatan. I had the opportunity to start my graduate school career at the same time he started at UW. While we experienced many growing pains that often come from a brand new lab, I was lucky enough to learn directly from him. His support kept me going when this project seemed like it was never going to work. I would also like to thank my committee members: Dustin Maly, Stefan Stoll, Wenqing Xu, and David Kimelman for their advice and support throughout my PhD pursuit.

I would like to thank my lab mates and graduate school friends. In particular, I would like to thank Dr. Betsy Speltz. She is one of the most intelligent, kind, and strong women I have ever had the pleasure to work with. I have an incredible amount of respect for her and I can only hope to be even a fraction of the scientist and woman she is. I would also like to thank Maire Gavagan. She joined the lab two years after me but I have learned so much from her and I know she will do amazing work in this field. To Chen Dong: I am so glad we joined this lab together and I have thoroughly enjoyed getting to know him over these past five years. My lab mates in general are so fun and they let me drag them out into the world for lab bonding and celebrating every birthday or silly holiday. I was also lucky enough to meet many women in other chemistry disciplines who continue to inspire me both in and outside the lab: Emily Dieter, Chloe Humphries, and Beth Mundy.

I need to give a huge thanks to the friends who have stuck by me through so many years of high school and college: Erin Verdi, Megan Reinikka, Rachel Alley, Kelsey Arroyo, and Catherine Walker. They are the best friends anyone could ever hope to have. I would also like to thank the newest addition to my life: Max Lee. He is a never-ending fountain of support, he always celebrates

the highs, and comforts me during the lows. I am so incredibly grateful to have him in my life and I am so excited for our next adventure together.

Finally, I would not have finished graduate school without the endless support of my family. The Fagnans know how to throw a party and they always made sure I left with loads of leftovers. The Unruhs and Crabtrees brought the fun and I loved getting my graduate school frustrations out with very competitive card games. Thank you to my brother, Matthew, who is much smarter than I am and has always been my friendly competition. Without him, I would not have pushed myself in school as much as I did. The biggest thanks I can give go to my parents, Todd and Lori Fagnan. Thank you for picking me up late at night so that I didn't have to take the bus. Thank you for moving me every single year. And thank you for all of the grocery store runs. Thank you so much for always supporting my dreams and making sure I had everything I could ever need.

Chapter 1. Introduction

Cells receive a constant influx of signals, such as growth factors and hormones that activate specific pathways. The cell must integrate the wide range of incoming signals and coordinate the activated pathways, resulting in a varied range of responses. While there are many pathways and networks specific to a cellular function, most signaling pathways are not completely insulated from each other. There are many proteins that have activity across several pathways and function in a variety of contexts.[1–4] Since these proteins are activated with multiple inputs, the cell must maintain tight control with a high level of specificity. To date there has been a large body of work using genetics and cell biology to investigate how cells are able to function with these shared proteins and integrate multiple inputs without activating the incorrect pathway. Despite all of this work, we still do not fully understand the fundamental molecular events behind how cells are able to achieve the level of specificity needed to maintain proper function.

1.1 Scaffold Protein Function and Regulation

One strategy for specificity is the spatial organization of distinct subsets of signaling proteins on a scaffold protein.[5] Scaffold proteins are classically defined as binding platforms that assemble signaling components into larger complexes that mediate pathway outputs.[6] Not only do scaffolds assemble these signalosomes, they also can localize the complexes to specific cellular locations.[7–12] Additionally, it is widely accepted that as a consequence of assembling signaling complexes, scaffold proteins enhance kinase activity and increase reaction rates. For example, Ste5, a model scaffold within the yeast mating pathway, adopts different conformations to either prevent or

enhance the phosphorylation of the mitogen activated protein kinase (MAPK) Fus3.[13,14] Kinase suppressor of Ras (KSR), a scaffold within the extracellular signal-regulated (ERK) pathway, is not necessary for signaling but has a major role in increasing the efficiency and specificity of kinase activity as well as modulating the duration and intensity of signaling.[12,15–17] Scaffold proteins can also recruit negative regulatory machinery. For example, the c-Jun N-terminal kinase (JNK) scaffold, JNK interacting protein (JIP-1), recruits both the upstream activating kinases (MAPKK and MAPKKK) and the inactivating phosphatase.[18,19] AKAPs also recruit phosphodiesterases which break down cAMP (cyclic adenosine monophosphate) to create a locally inactive pool of protein kinase-A (PKA).[20,21] These types of assemblies create an additional layer of control over pathway signaling responses either through duration of signaling or magnitude of the signal.

In addition to binding kinase cascades and their regulatory machinery, scaffolds can also be targets for direct regulation. This is another useful and efficient signaling tool because the modification of a single protein can regulate an entire pathway. A common regulatory modification is phosphorylation. For example, in T-cell signaling the scaffold LAT is not phosphorylated until the pathway is activated. Upon phosphorylation LAT can then assemble an active signaling complex, and thus activate downstream T-cell activation pathways.[15,22] On the other hand, phosphorylation of the scaffold Ste5 is an inhibitory event that actually prevents the mating pathway from proceeding.[23]

The first descriptions of scaffold proteins focused on the idea that scaffold proteins function to increase reactions rates. However, it is becoming increasingly evident that scaffold proteins may

work to regulate kinase activity in a variety of ways, some of which are described above. Despite the large body of work that is based on the assumption that scaffold proteins enhance reaction rates, there is a surprising lack of kinetic analysis of these scaffold-mediated effects. An in-depth analysis of *in vitro* kinetic parameters within a well-defined model is necessary to determine what the extent of scaffold-mediated rate enhancement is and how regulation of scaffolds contributes to this effect.

1.2 Study of Scaffold Function Within the Wnt Signaling Pathway

1.2.1 *The Wnt Pathway and the Central Scaffold Axin*

The complex network of developmental signaling pathways is an interesting system to investigate the catalytic nature of scaffold proteins. In particular, the Wnt signaling pathway makes for a unique and medically relevant system for studying scaffold-mediated rate enhancements because it contains many scaffolds and many multi-functional proteins that are involved in many other pathways. The core reaction consists of the phosphorylation of β-catenin by glycogen synthase kinase 3β (GSK3β).[24–26] β-catenin must first undergo a priming phosphorylation by casein kinase I alpha (CKIα).[27] These proteins are assembled onto the scaffold Axin, along with many others, to form the destruction complex. In the absence of a Wnt signal, the destruction complex facilitates the phosphorylation of β-catenin, marking it for degradation (Figure 1.1A). When an extracellular Wnt ligand binds its membrane receptors Frizzled (Fz) and lipoprotein receptor-related protein (LRP), the destruction complex is recruited to the membrane via another scaffold protein Dishevelled (Dvl). Upon recruitment to the membrane, GSK3β activity is inhibited through an unknown mechanism and can no longer phosphorylate β-catenin. The cytosolic concentration of

β-catenin increases and initiates transcription of Wnt target genes (Figure 1.1B).[28] Aside from this general outline of the pathway, the precise mechanism of activation is still unknown.

1.2.2 *Models for Wnt Activation and the Role of Axin*

Interestingly, Axin is considered to be the rate-limiting component in the Wnt pathway because it

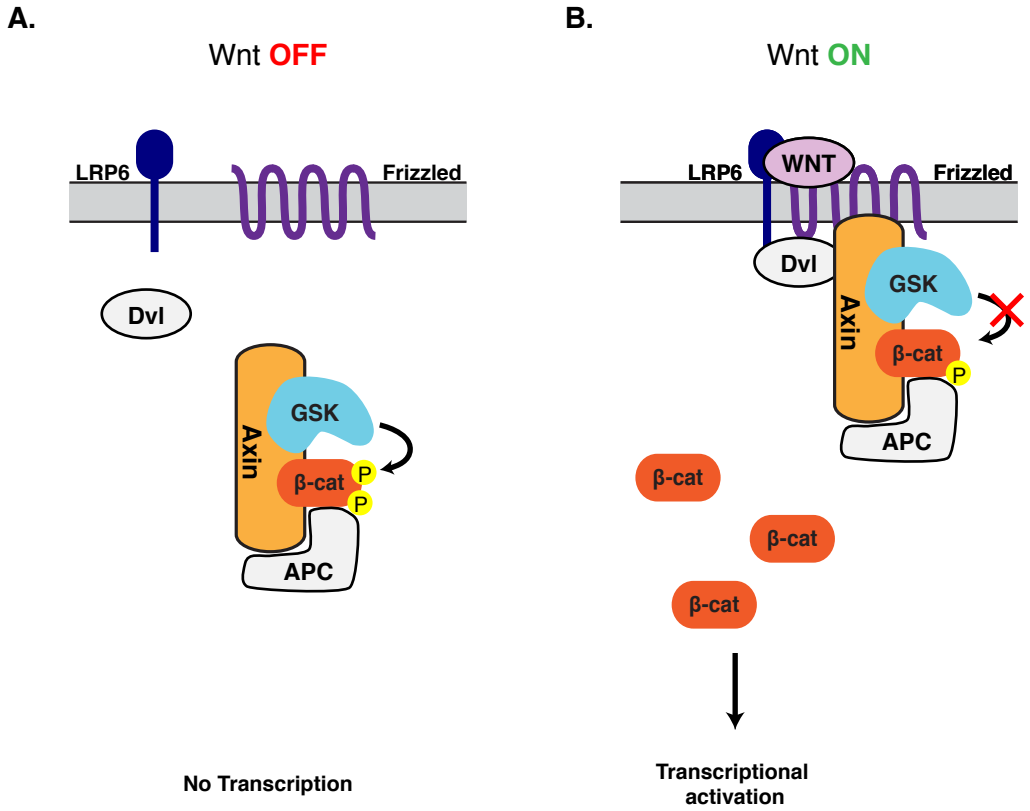

Figure 1.2 Wnt Signaling Pathway

(A) In the absence of Wnt signal the destruction complex is active. GSK3β phosphorylates β-catenin marking it for proteasomal degradation. (B) The destruction complex is recruited to the membrane via Dishevelled (Dvl), another Wnt scaffold protein. GSK3β no longer phosphorylates β-catenin which allows it to accumulate within the cell and initiate a Wnt- dependent transcriptional response.

exists at such a low concentration within the cell.[29,30] In addition to this low concentration, there is a significant amount of evidence from mutational studies that also point to the importance of Axin. It's incredibly difficult to study Axin knockouts because they are embryonic lethal in mice. However certain mutations in the gene that codes for Axin revealed that Axin is vital in regulating the Wnt pathway and normal development.[31] Additionally, mutations in Axin that abolish the β-catenin binding site have been identified in several human liver cancers.[32] All of this evidence suggests that Axin is one of the central pathway proteins and may play a significant role in the Wnt pathway. There are many models for Wnt pathway activation that center around the functions of the destruction complex and the role of Axin. These models are based on the assumption that the main role of Axin is to tether GSK3β and β-catenin together in order to increase the rate of phosphorylation. An implicit assumption in this is that by enhancing this reaction, Axin is directing GSK3β activity specifically to the Wnt pathway.

Inactive Destruction Complex is Retained at the Membrane- When the destruction complex is recruited to the membrane upon Wnt binding, GSK3β phosphorylates the cytosolic tail of the transmembrane protein LRP which forms a pseudo-substrate for GSK. The newly phosphorylated tail binds GSK and prevents further phosphorylation and subsequent proteasomal degradation of β-catenin (Figure 1.2A).[33,34] This model is often referred to as the "Biochemical Model" because a vast majority of the supporting literature is based on *in vitro* experiments using fusion proteins and high protein concentrations.[35] Since most of the core signaling components have low cellular concentrations,[36] it is often challenged as not accurately representing the cellular environment.

Destruction Complex is Sequestered- In this model, once the destruction complex is recruited to the membrane it is endocytosed along with the Fz/LRP receptor complex into an early endosome vesicle that eventually fused with a multivesicular body (Figure 1.2B).[37] The destruction complex is physically sequestered from the signaling components in the cytosol by a double-membrane layer so that GSK3β can no longer phosphorylate newly synthesized β-catenin. This results in the accumulation of β-catenin within the cell.

Disassembly of the Destruction Complex- There are several models that propose that some component of the destruction complex dissociates thus rendering the destruction complex non-functional. For example, direct binding of Axin and Dvl through the DIX domain is thought to break-up the destruction complex upon Wnt pathway activation.[38–40] Additionally, Frat and GBP proteins may disrupt the destruction complex through competition with Axin for binding to GSK3β.[41–43] Finally, the destruction complex may dissociate through the direct regulation of Axin.

Axin Adopts an Auto-Inhibited State- As previously described, Axin is an example of a scaffold that assembles both activating and inhibitory signaling components. In the absence of a Wnt signal, Axin is phosphorylated in a GSK3β/CKI-dependent manner. This phosphorylation event allows Axin to adopt a conformation that can then bind β-catenin and allow for phosphorylation by GSK3β. When Axin is recruited to the membrane upon Wnt ligand binding, Axin is dephosphorylated by another component of the complex, the phosphatase PP1. When Axin is no longer phosphorylated, it adopts a conformation that no longer productively binds β-catenin which results in cytosolic accumulation (Figure 1.2C).[44] Interestingly, when this dephosphorylation is blocked, the Wnt pathway is inhibited.[45]

While this discussion is by no means comprehensive, it does describe some of the common themes of pathway activation in the Wnt signaling field. In particular, these models implicitly suggest that the phosphorylation of β-catenin is significantly faster in the presence of the destruction complex. In all of these models, Wnt activation is characterized by a decrease in β-catenin phosphorylation. If the rate of phosphorylation remained the same, then we would still see β-catenin phosphorylation by GSK3β even in the absence of the destruction complex. It is only because of the regulation by the destruction complex that we are able to see a difference in phosphorylation between Wnt on and off states.

1.3 Wnt Signaling and Disease

The Wnt pathway is highly interconnected and is linked to numerous diseases, particularly cancer.[3,28,46,47] Mutations in core signaling components, such as Axin, β-catenin, and APC are strongly linked to a variety of cancers, especially colon cancer and hepatocellular carcinomas.[32,48,49] Interestingly, many of these mutations result in truncations that abolish binding sites for other destruction complex signaling components. Additional studies of mutations in the

Fused locus of mice showed that mutations in Axin often resulted in cardiac and

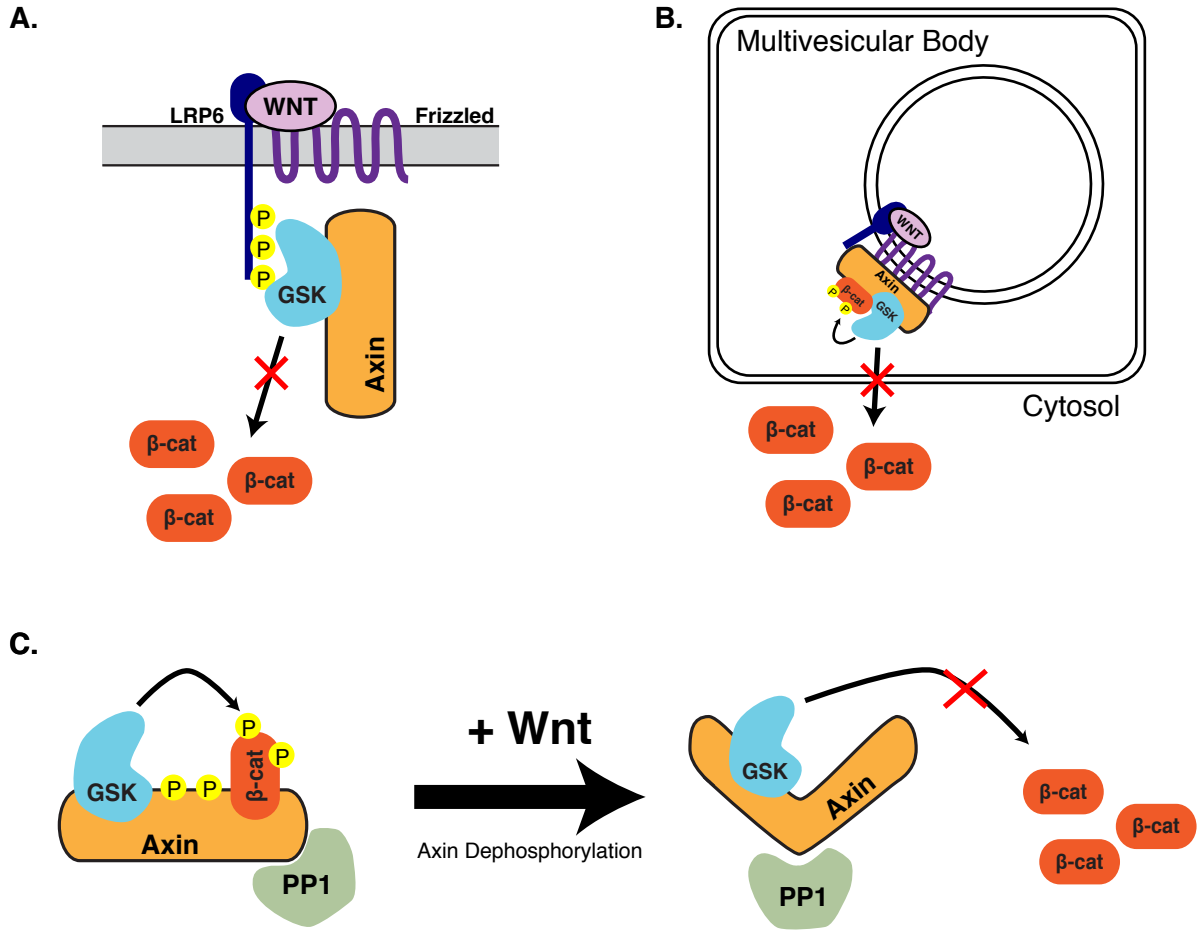

Figure 1.3 Models for Wnt Pathway Activation

(A) Upon Wnt binding to the receptors, the destruction complex is recruited to the membrane and subsequently trapped in an inactive state through competitive inhibition of GSK3β. (B) The destruction complex is endocytosed into a vesicle along with the Wnt receptors. The destruction complex is physically blocked from accessing newly synthesized β-catenin. (C) In the absence of a Wnt signal Axin is phosphorylated and able to bind β-catenin. In the presence of a Wnt signal Axin is dephosphorylated and can no longer bind β-catenin, resulting in the cytosolic accumulation of β-catenin.

developmental abnormalities.[31] Mutations in many of the Wnt ligands, receptors, and pathway regulators are often seen in degenerative diseases that result in abnormalities in bone density, tooth

development, and the retina.[28] Because of this, the Wnt pathway is often the target for medical treatment. However, due to the many connections with other pathways it has been difficult to develop targeted and effective treatments. For example, one target for cancer treatment is a Porcupine o-acyltransferase (PORCN) which is a protein responsible for the secretion of Wnt ligands. However, small molecule inhibitors of PORCN often results in bone toxicity.[50] Understanding the molecular mechanism of Wnt pathway activation is vital to the development of more effective treatments with less off target effects. Not only will this be useful in drug development, but it will also provide context for stem cell biology and regenerative medicine. The Wnt pathway is an important component in stem cell biology and a more thorough understanding of the pathway will assist in developing tools to further study stem cells and their use in tissue regeneration.[28]

It is clear from the variety of activation models (described above) that there is no well-defined mechanism for Wnt pathway activation. This is an especially interesting problem because the Wnt pathway has many connections to other signaling networks. We still do not understand the precise mechanism of pathway activation and disruption of GSK3β activity. Nor do we understand how multi-functional proteins within this pathway, such as GSK3β, are able to maintain specificity so as not to misactivate another connected pathway. The lack of this knowledge presents a common challenge in developing treatments that target Wnt pathway proteins, or any multifunctional proteins, with a degree of specificity that would prevent any off-target effects. My work describes efforts to biochemically reconstitute the core reaction in the destruction complex *in vitro* to better understand how, or if, scaffold proteins function to promote specificity of kinase reactions within the Wnt pathway.

Chapter 2. The Wnt pathway scaffold protein Axin promotes signaling specificity by suppressing competing kinase reactions

2.1 Introduction

GSK3β is a central kinase in mammalian cell signaling networks that responds to growth factors and hormones to regulate cell growth, differentiation, and metabolism.[51] GSK3β receives signals from multiple upstream inputs and acts on several distinct downstream protein targets (Figure 2.1A). GSK3β-dependent responses to Wnt and growth factor or insulin signals appear to be insulated from each other, so that Wnt signals do not activate a growth factor/insulin response and vice versa.[52–54] These observations raise the fundamental question of how GSK3β activity can be independently regulated by different signaling pathways. Analogous questions arise in many eukaryotic signaling networks, and understanding the mechanisms by which biochemical systems resolve this problem is a major outstanding challenge for the field.

Scaffold proteins that physically assemble protein signaling pathways provide potential mechanisms to direct shared signaling proteins to specific downstream targets.[5,13,55] In the Wnt signaling network, the scaffold protein Axin coordinates the assembly of a multi-protein complex including GSK3β and its substrate β-catenin.[28] By binding to both GSK3β and β-catenin, Axin is thought to promote β-catenin phosphorylation.[56–58] Consequently, regulation of Axin provides a possible mechanism to control GSK3β activity towards β-catenin without affecting GSK3β reactions towards other, non-Wnt pathway substrates.[4]

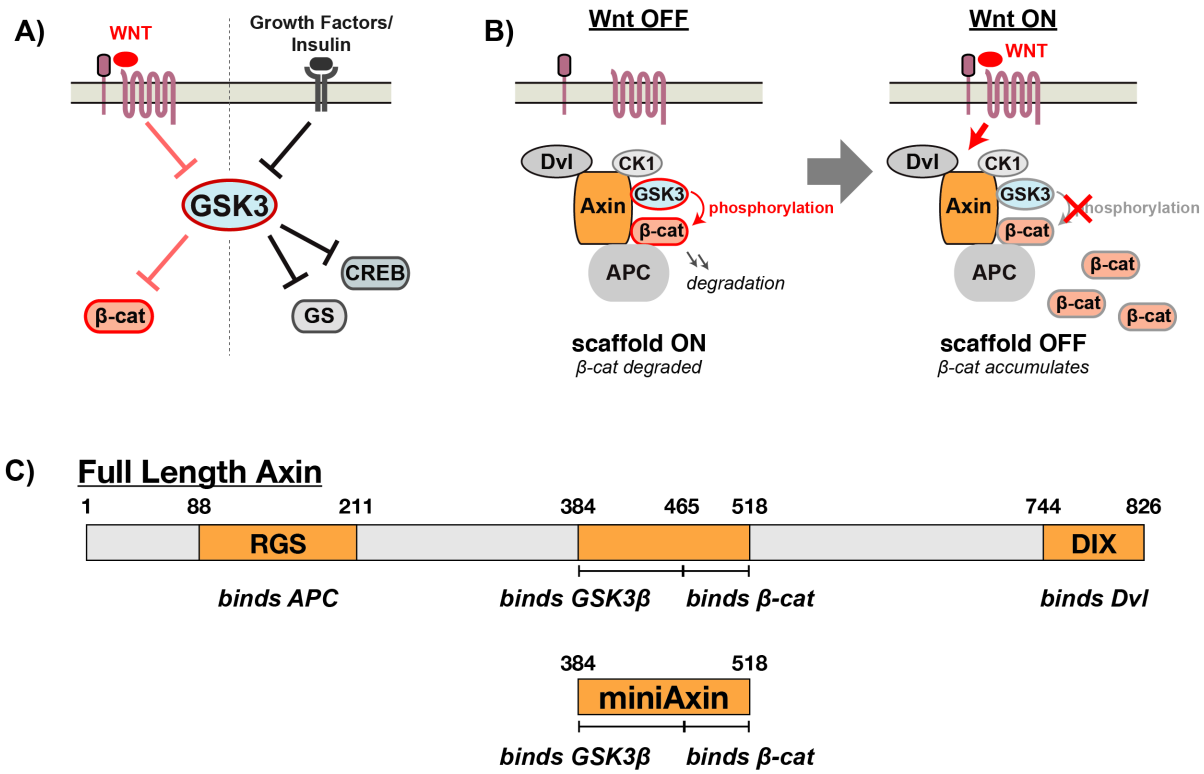

Figure 2.1 Axin assembles signaling proteins in the Wnt pathway.

(A) GSK3β receives input signals from Wnt, growth factors, and hormones like insulin and responds by acting on multiple distinct downstream targets. Wnt signals appear to be insulated from growth factor/insulin signaling. (B) GSK3β assembles into a multi-protein destruction complex with β-catenin, CK1α, Axin, Dvl, and APC. In the absence of a Wnt signal, β-catenin is phosphorylated and degraded. In the presence of a Wnt signal, β-catenin phosphorylation is blocked, which allows β-catenin to accumulate. (C) Schematics of full length human Axin (isoform 2, Uniprot O15169-2) and $Axin_{384\text{-}518}$ (miniAxin), which contains the binding sites for both GSK3β and β-catenin (see Methods for an explanation of domain boundaries).

We know a great deal about the general features of Wnt pathway activation, although controversy remains surrounding the molecular mechanisms by which Wnt signaling controls β-catenin phosphorylation and the precise role of Axin in this process.[28] In the absence of a Wnt signal, β-catenin is sequentially phosphorylated by the kinases CK1α and GSK3β, which leads to proteasomal degradation of β-catenin (Figure 2.1B). The phosphorylation reaction takes place in a multi-protein destruction complex that includes the scaffold protein Axin, the kinases CK1α and

GSK3β, the substrate β-catenin, and the accessory proteins Dvl and APC, which may also have scaffolding functions. Wnt pathway activation disrupts the activity of the destruction complex, allowing β-catenin to accumulate and activate downstream gene expression. Wnt signaling has been proposed to block β-catenin phosphorylation at both the CK1α and GSK3β kinase reaction steps,[59] possibly via a phosphorylation-dependent conformational change in Axin.[44] An alternative proposal suggests that Wnt signals interfere with the β-catenin ubiquitination step.[60]

Initial support for the model that Axin promotes β-catenin phosphorylation came from *in vitro* biochemical experiments showing that the rate of GSK3β-catalyzed β-catenin phosphorylation increases substantially in the presence of Axin.[56–58] To test this hypothesis, we biochemically reconstituted GSK3β-catalyzed reactions *in vitro* and quantitatively measured reaction rates in the presence and absence of the Axin scaffold protein. By defining a minimal kinetic framework and systematically measuring rate constants for individual reaction steps, we expected to determine whether Axin promotes binding between GSK3β and β-catenin or whether Axin allosterically modulates the activity of a GSK3β•β-catenin complex. Both mechanisms have been observed with other kinase signaling scaffolds,[5] and distinguishing between these possibilities is an important step towards understanding how Wnt signals might perturb Axin to regulate β-catenin phosphorylation.

Surprisingly, we found that Axin has small, ~2-fold effects on the steady state rate constants for β-catenin phosphorylation *in vitro*. We observed similar effects with CK1α-phosphoprimed β-catenin, which is the preferred substrate of GSK3β *in vivo*,[27,61] and with unprimed β-catenin, which was used in early biochemical studies.[56–58] We can find conditions where Axin produces relatively

large increases in observed rates, but this effect arises from an unexpected oligomerization event that occurs only in the unprimed reaction. At high concentrations of GSK3β, an inactive, oligomeric complex of GSK3β and β-catenin accumulates, and Axin prevents the formation of this inactive complex. This effect results from altering the accessibility of an active enzyme-substrate complex, not from tethering enzyme and substrate together. No corresponding inactive complex forms in the GSK3β reaction with CREB, a non-Wnt pathway substrate, and Axin actually decreases the rate of CREB phosphorylation ~35-fold. The ability of Axin to suppress a competing reaction provides a new potential mechanism for how scaffold proteins can promote specific reactions. Together, these data reveal important new biochemical features of the destruction complex, and models for Wnt pathway activation should be reassessed in light of the finding that Axin-mediated tethering is not sufficient to promote the reaction of GSK3β with β-catenin. Other Wnt pathway proteins may have important and as-yet-unrecognized roles in regulating and modulating GSK3β activity towards β-catenin without directly affecting other GSK3β targets.

2.2 Results

2.2.1 *Reconstituting a minimal destruction complex*

To test the model that Axin accelerates the reaction of GSK3β with β-catenin (Figure 2.2), we biochemically reconstituted a minimal reaction system for quantitative kinetic analysis. We purified recombinant human forms of GSK3β, phosphoprimed β-catenin, and Axin as maltose binding protein (MBP) fusions. We purified active GSK3β from *E. coli*[62] and found that it was phosphorylated on the activation loop Tyr216 (Figure S2.2A), as had been previously reported for GSK3β purified from insect cells.[56] We purified recombinant human phosphoprimed β-catenin

from *E. coli* by coexpressing β-catenin with CK1α (Figure S2.2)

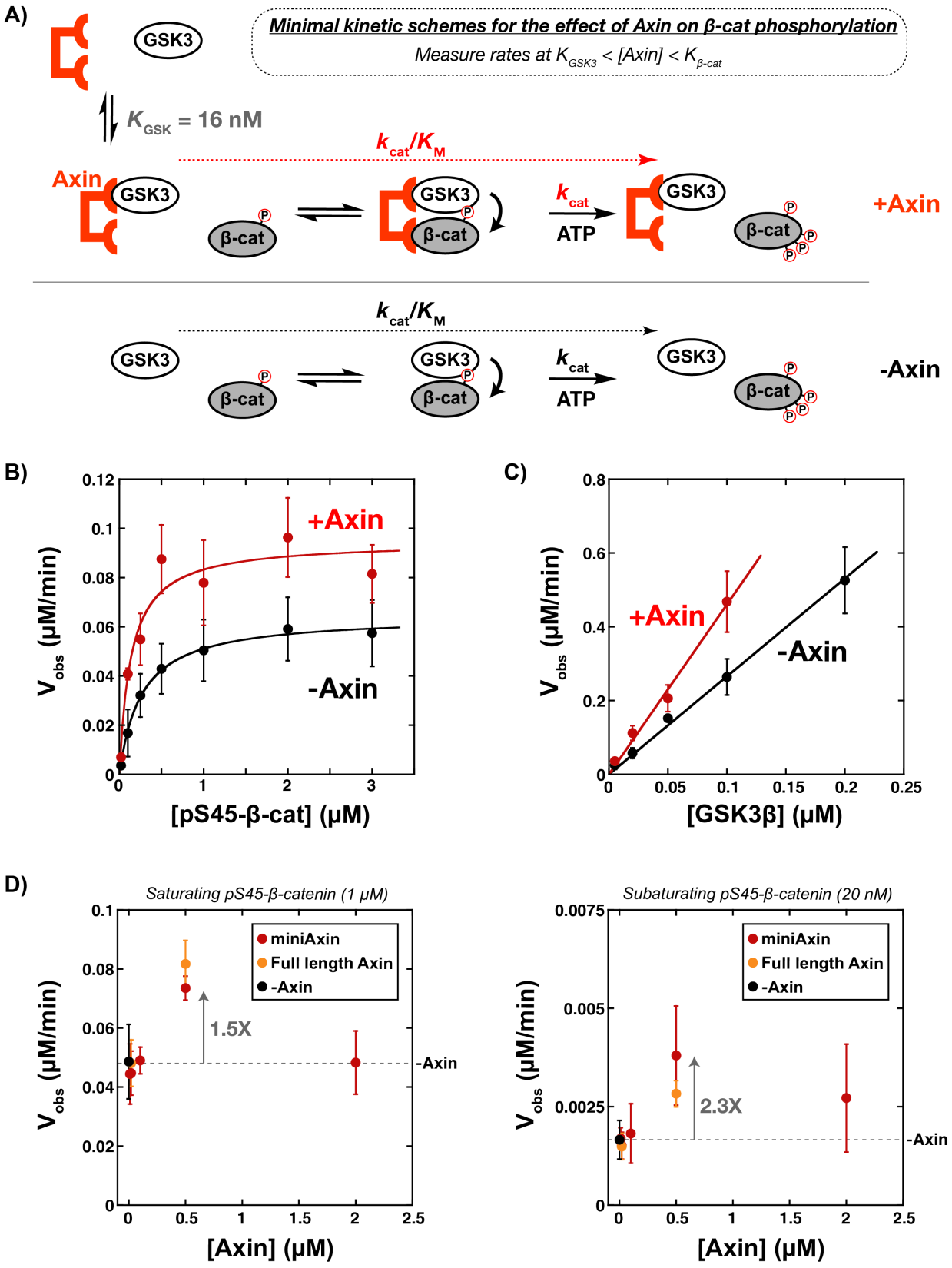

Figure 2.2 Axin has a modest effect on phosphorylation of phosphoprimed β-catenin.

(A) Minimal kinetic scheme for the reaction of GSK3β with pS45-β-catenin in the presence and absence of Axin. GSK3β phosphorylates pS45-β-catenin at three sites: S33, S37, and T41. When the Axin concentration is larger than the affinity for GSK3β (K_{GSK3}) but smaller than the affinity for pS45-β-catenin ($K_{\beta\text{-cat}}$), all GSK3β is bound to Axin (when [Axin] > [GSK3β]). By varying the concentration of pS45-β-catenin, we can obtain the Michaelis-Menten kinetic parameters k_{cat}, K_M, and k_{cat}/K_M for the reaction with the Axin•GSK3β complex. These parameters can be compared directly to the corresponding parameters for the reaction in the absence of Axin. (B) Michaelis-Menten plot of V_{obs} vs. [pS45-β-catenin] at 20 nM GSK3β in the presence and absence of 500 nM miniAxin. See Table 2 for values of fitted kinetic parameters. (C) Plot of V_{obs} vs. [GSK3β] at 1 μM pS45-β-catenin in the presence and absence of 500 nM miniAxin. V_{obs} increases linearly with enzyme concentration, as expected. An accurate initial rate for 0.2 μM GSK3β with Axin could not be measured because the reaction exceeded 40% conversion before two timepoints could be collected. (D) Plots of V_{obs} vs. [Axin] with either miniAxin or full length Axin, 20 nM GSK3β, and 1 μM or 20 nM pS45-β-catenin. It is important to test both saturating concentrations (i.e. k_{cat} conditions, 1 μM pS45-β-catenin) and subsaturating concentrations (i.e. k_{cat}/K_M conditions, 20 nM pS45-β-catenin) because if Axin has a large effect on K_M it would not be detectable in saturating conditions. For full length Axin, only a subset of Axin concentrations were measured (20 and 500 nM). Error bars in (B)-(D) are mean ± SD for at least 3 measurements.), which produces phospho-Ser45 β-catenin (pS45-β-catenin). For comparison, we purified unprimed β-catenin expressed in the absence of CK1α. Finally, we purified full length Axin and a minimal fragment of Axin (miniAxin, residues 384-518) that includes the domains that bind both GSK3β and β-catenin (Figure 2.1C).[56,63]

To confirm that recombinant Axin binds GSK3β and β-catenin in our *in vitro* system, we performed quantitative binding assays using bio-layer interferometry. We determined that Axin has a K_D of 7.5 nM for GSK3β (Figure 2.2A and Table 1). The miniAxin fragment has a K_D of 16 nM for GSK3β. These values are similar to the previously reported K_D of 65 nM for the interaction between human GSK3β and rat Axin.[58] Because miniAxin behaved similarly to full length Axin, and because this construct was easier to express and purify in larger quantity than the full length protein, we used miniAxin for most subsequent binding and kinetic assays. For several key experiments, we verified that full length Axin gave similar behavior.

Table 1 Binding constants for Axin interacting with GSK3β and β-catenin[a]

Immobilized Substrate	Binding Partner	K_D	k_a ($M^{-1}s^{-1}$)	k_d (s^{-1})
miniAxin	GSK3β	16 nM	1.7×10^4	2.7×10^{-4}
Axin (full length)	GSK3β	7.5 nM	2.7×10^4	2.0×10^{-4}
AxinΔBCD	GSK3β	11 nM	1.9×10^4	2.1×10^{-4}
pS45-β-catenin	miniAxin	12 μM	6.4×10^3	7.3×10^{-2}

[a] Binding constants were determined using bio-layer interferometry as described in the Methods. See Figure S2.2. All fits had χ^2 values < 1 and R^2 values > 0.98.

We proceeded to measure the affinity of miniAxin for pS45-β-catenin. The observed K_D of 12 μM (Figure S2.2B) is somewhat weaker than the reported K_D of 1.6 μM for unprimed mouse β-catenin binding to a short human Axin fragment (residues 436-498).[64] We could detect miniAxin binding to unprimed β-catenin in a similar concentration range, but we were unable to accurately measure a K_D value due to surface aggregation artifacts. Taken together, we confirmed that Axin binds both GSK3β and β-catenin, and that the affinity of Axin for GSK3β is substantially tighter than that for β-catenin.

To determine how Axin affects the β-catenin phosphorylation reaction, we defined a minimal, simplified kinetic scheme to directly compare values of the steady state rate constants k_{cat}/K_M and k_{cat} in the presence and absence of Axin (Figure 2.2A). Because Axin binds GSK3β much more tightly than β-catenin, we worked at a fixed Axin concentration where GSK3β is fully bound and measured rates vs. β-catenin concentration. If Axin promotes binding between GSK3β and β-catenin, the observed K_M should shift to a lower concentration and k_{cat} should remain unchanged

(i.e. the bimolecular rate constant k_{cat}/K_M would increase). Alternatively, if Axin allosterically activates the GSK3β•β-catenin complex, then k_{cat} should increase without necessarily affecting K_M.

To measure β-catenin phosphorylation rates, we used quantitative Western blotting. GSK3β sequentially phosphorylates pS45-β-catenin at three sites: T41, S37, and S33,[27] and product formation can be monitored using an antibody specific for pS33/pS37/pT41-β-catenin (see Methods). In the presence of miniAxin, we observed a 1.5-fold increase in k_{cat}, a 2-fold decrease in K_M, and a 3-fold increase in k_{cat}/K_M (Figure 2.2B & C, Table 2). These effects are far smaller than expected based on prior reports, one of which suggested that Axin accelerates the reaction by $>10^4$-fold.[56–58]

Table 2 Kinetic parameters for GSK3β reactions.[a]

Substrate	Reaction	k_{cat} (s^{-1})	K_M (μM)	k_{cat}/K_M ($M^{-1}s^{-1}$)
pS45-β-catenin	–Axin	$(5.4 \pm 0.1) \times 10^{-2}$	0.26 ± 0.02	$(2.0 \pm 0.2) \times 10^5$
	+Axin	$(7.9 \pm 0.6) \times 10^{-2}$	0.14 ± 0.05	$(5.7 \pm 2.0) \times 10^5$
β-catenin	–Axin	$(1.3 \pm 0.04) \times 10^{-4}$	0.034 ± 0.004	$(3.7 \pm 0.4) \times 10^3$
	+Axin	$(1.5 \pm 0.09) \times 10^{-4}$	0.031 ± 0.007	$(4.9 \pm 1.2) \times 10^3$
pS133-$CREB_{127-135}$	–Axin	$(1.0 \pm 0.2) \times 10^{-3}$	0.10 ± 0.06	$(9.8 \pm 6.4) \times 10^3$
	+Axin[b]	n.d.	n.d. ($\geq$0.5 μM)	$(2.8 \pm 0.1) \times 10^2$

[a] All +Axin reactions were measured with the miniAxin construct (Table 3). See Figures 2.2, 2.3, and 2.5 for data and the Methods section for the kinetic model used to fit the data. Standard errors for k_{cat} and K_M are from non-linear least squares fits to the initial rate data. The error for k_{cat}/K_M is propagated from the individual k_{cat} and K_M values.

[b] The CREB reaction in the presence of Axin did not detectably saturate up to 0.5 μM pS133-$CREB_{127-135}$ (Figure 2.5B). Only the value of k_{cat}/K_M could be obtained.

We considered several possible explanations for the discrepancy between our results and prior work. First, scaffold-dependent reactions can be slow if too little scaffold is present, but inhibited at excess scaffold concentrations if the kinase and substrate are not bound to the same scaffold.[65] To test this possibility, we varied the concentration of miniAxin and measured reaction rates at both saturating and subsaturating pS45-β-catenin concentrations, but found no miniAxin concentration that produced a larger rate enhancement (Figure 2.2D). Second, it is possible that the miniAxin fragment lacks some important functional domain. When we measured reaction rates in the presence of full length Axin, however, there was no significant difference compared to miniAxin (Figure 2.2D). Thus, Axin has only a modest effect on the GSK3β reaction with pS45-β-catenin, and this effect arises from small changes in both k_{cat} and K_M. The decrease in K_M suggests that Axin promotes binding between GSK3β and pS45-β-catenin by a factor of ~2-fold. The effect is relatively small, possibly because Axin binding to β-catenin is weak (K_D ~12 μM) compared to the K_M for the reaction of GSK3β with pS45-β-catenin (K_M = 0.26 μM). In order to obtain large tethering effects from a scaffold, it may be necessary for binding affinities to the scaffold to be at least comparable to the un-scaffolded interaction between kinase and substrate, or for ternary complex formation to be highly cooperative (Speltz and Zalatan, manuscript in preparation).

2.2.2 *GSK3β reactions with unprimed β-catenin*

The initial biochemical studies on Axin were performed with unprimed β-catenin as a substrate,[56–58] prior to or concurrent with the discovery of phosphopriming by CK1.[27,61] One early mechanistic model for Axin suggested that its function might be to bypass the need for phosphopriming.[66] In this case, either phosphopriming of β-catenin or Axin-mediated tethering would promote the

reaction of GSK3β with β-catenin, but there might not be an additional effect from Axin when β-catenin is phosphoprimed. When we measured reaction rates with unprimed β-catenin, however, we found that miniAxin had no significant effect on reaction rates (Figure 2.3A & B, Table 2). Varying the miniAxin concentration did not produce significant rate effects (Figure 2.3C). Thus, it appears that Axin-mediated tethering does not enhance the reaction of GSK3β with unprimed β-catenin.

Because CK1α-phosphoprimed β-catenin is the preferred substrate for GSK3β *in vivo*, we expected that the reaction of GSK3β with pS45-β-catenin should be significantly faster than the reaction with unprimed β-catenin. As expected, the value of k_{cat}/K_M for phosphoprimed β-catenin was ~10^2-fold larger than that for unprimed β-catenin, and this effect was independent of the presence of Axin (Table 2). This result is consistent with *in vitro* studies of the reaction of GSK3β with glycogen synthase, where GSK3β activity is undetectable unless glycogen synthase is phosphoprimed.[67]

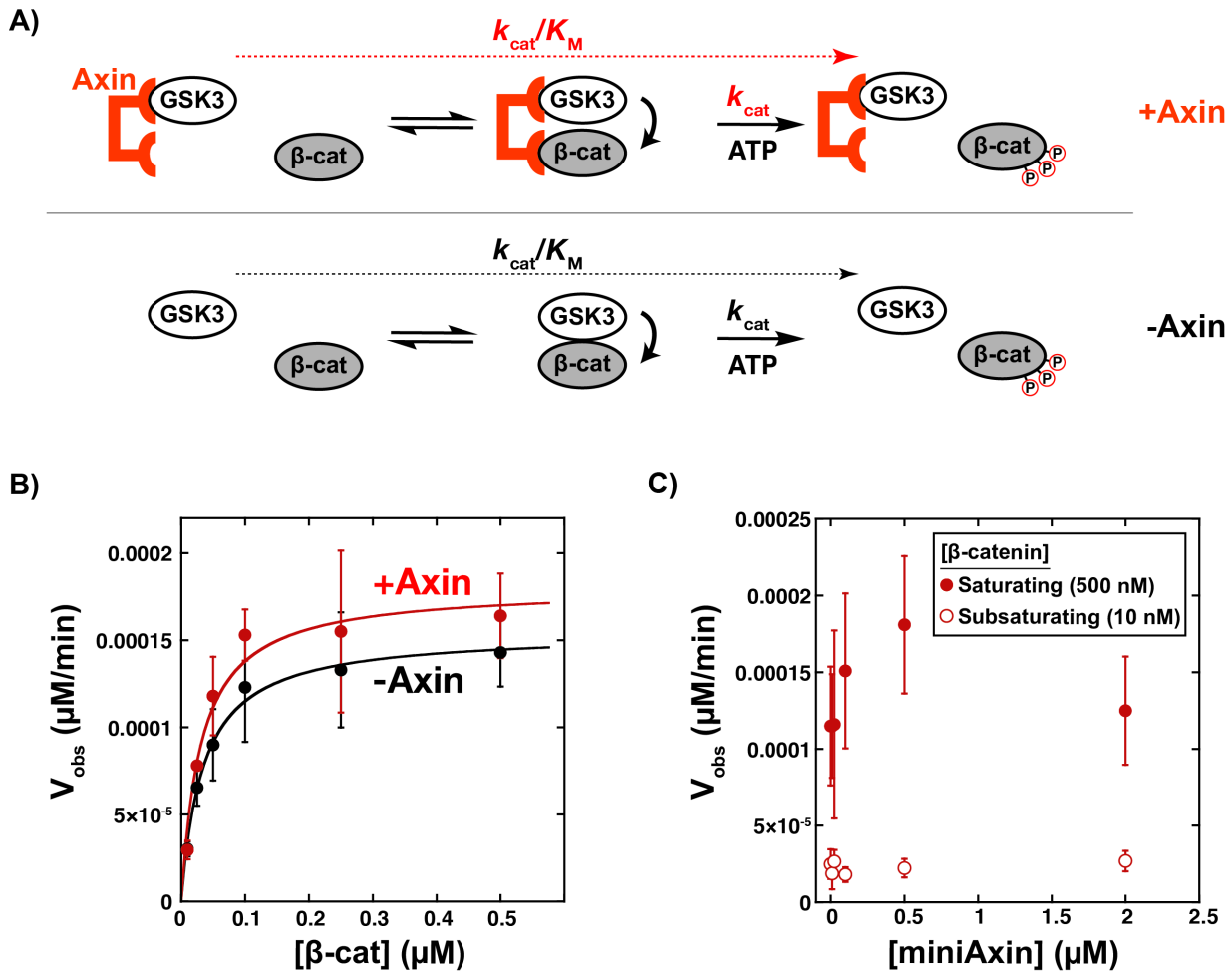

Figure 2.3 Axin has no significant effect on phosphorylation of unprimed β-catenin.

(A) Minimal kinetic scheme for the reaction of GSK3β with β-catenin in the presence and absence of Axin, following Figure 2.2A. GSK3β phosphorylates β-catenin at three sites: S33, S37, and T41. (B) Michaelis-Menten plot of V_{obs} vs. [β-catenin] at 20 nM GSK3β in the presence and absence of 500 nM miniAxin. The observed rates and rate constants in the presence and absence of Axin are indistinguishable within experimental error. See Table 2 for values of fitted kinetic parameters. (C) Plot of V_{obs} vs. [miniAxin] at 20 nM GSK3β and 10 nM (subsaturating) or 500 nM (saturating) β-catenin. Error bars in (B)-(C) are mean ± SD for at least 3 measurements.

2.2.3 *Axin rescues GSK3β from an inactive state*

Additional control experiments revealed an unexpected behavior that can explain previous reports of large Axin-mediated rate enhancements. In most circumstances, enzymatic reaction rates should increase linearly with increasing enzyme concentration, and this behavior is observed in the

reaction with pS45-β-catenin (Figure 2.2C). When we increased the GSK3β concentration in reactions with unprimed β-catenin, we observed that the rate does not increase linearly with GSK3β concentration. Instead, in the absence of Axin the observed rates level off sharply above ~100 nM GSK3β (Figure 2.4A & B). In contrast, in the presence of Axin the observed rates increase linearly with GSK3β concentration (Figure 2.4A). Thus, if reaction rates are measured at relatively high levels of GSK3β, which was the case in the early biochemical studies,[56–58] Axin produces a significant increase in the observed rates. Because the apparent inactivation of GSK3β is concentration dependent, the simplest model to explain this effect is that GSK3β forms an inactive dimer or oligomer and that Axin rescues GSK3β from this inactive state. There is evidence that GSK3β forms a dimer, and that Axin binding prevents GSK3β dimer formation.[42] Thus, Axin acts to maintain GSK3β in a kinetically active state.

The ability of Axin to stabilize an active state of GSK3β raises the question of whether the scaffolding function of Axin (i.e. binding both GSK3β and β-catenin) is necessary for its observed effect on GSK3β activity. Alternatively, the GSK3β binding function alone might be sufficient. To distinguish between these possibilities, we removed the β-catenin binding domain (BCD) from Axin (Figure S2.7) and assessed the effect of this AxinΔBCD mutant on GSK3β activity. The affinity (K_D) of GSK3β for AxinΔBCD was indistinguishable from that for full length Axin (Table 2), but the activity of AxinΔBCD was significantly impaired compared to full length Axin (Figure S2.7). Adding the BCD fragment back to an AxinΔBCD reaction in trans did not rescue the activity of AxinΔBCD (Figure S2.6). These experiments demonstrate that the ability of Axin to stabilize active GSK3β requires a scaffold that can interact with both GSK3β and β-catenin. Further, they suggest that the inactive state of GSK3β may not be composed of GSK3β alone. Instead, the

inactive state is a dimeric or oligomeric form of the GSK3β•β-catenin complex that accumulates at high GSK3β concentration.

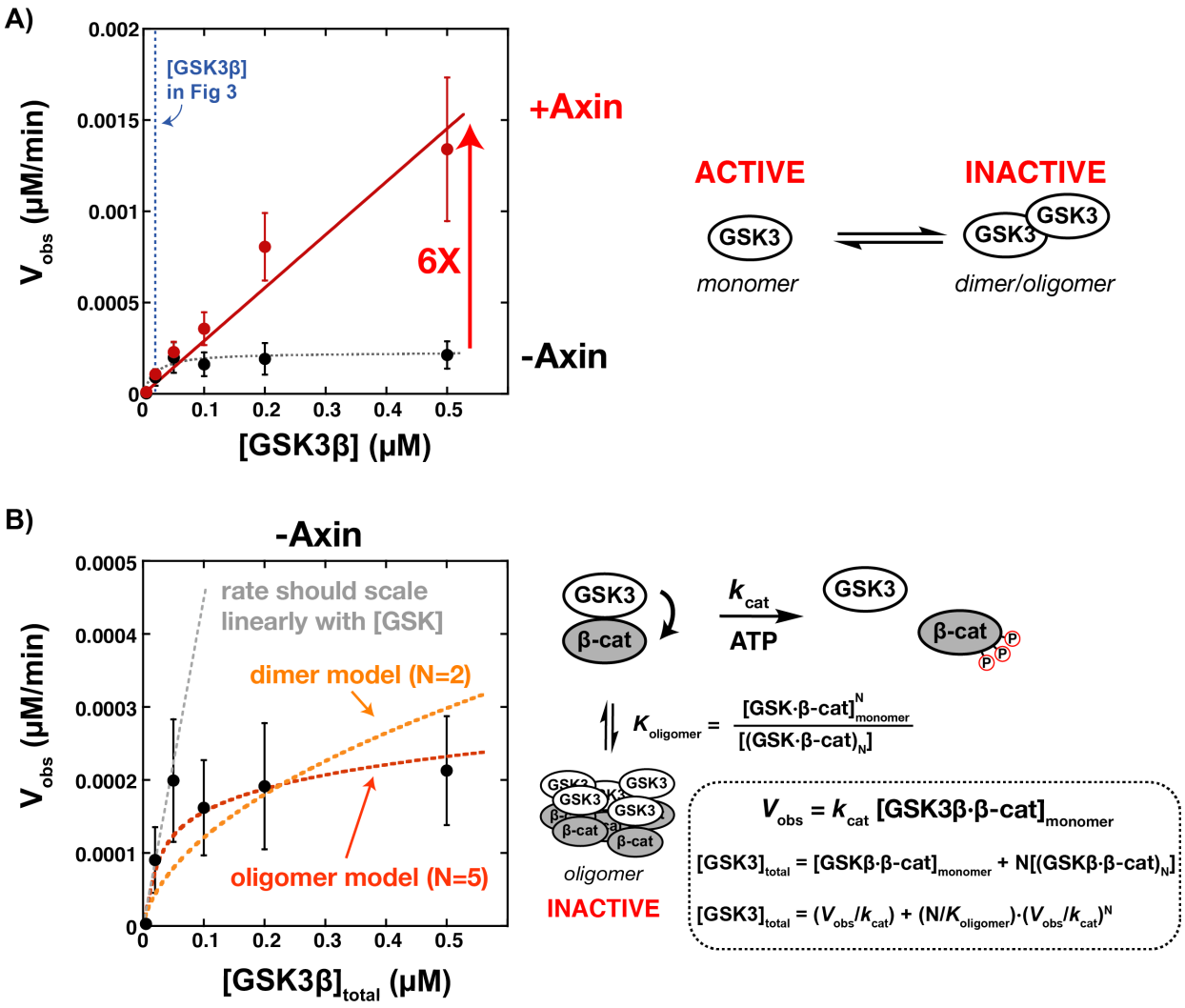

Figure 2.4 Axin rescues GSK3β from an inactive state.

(A) Plot of V_{obs} vs. [GSK3β] at 500 nM β-catenin in the presence and absence of 500 nM miniAxin. (B) Expanded view of the plot of V_{obs} vs. [GSK3β] in the absence of Axin, and a kinetic model with an inactive, oligomeric state. In the absence of the inactive state, V_{obs} should increase linearly with [GSK3β]. Fitting the data to a model with an inactive GSK3β dimer (N=2) gives non-linear behavior but still shows substantial deviations from the data. Fitting the data to a model with a higher-order inactive GSK3β dimer (N=5) gives a reasonable fit. Larger values of N give indistinguishable fits to the data. Error bars in both panels are mean ± SD for at least 3 measurements.

Further characterization revealed two additional important features of this unusual active/inactive transition of GSK3β. First, to distinguish between a reversible or irreversible transition, we initiated a reaction at high GSK3β concentration in the absence of Axin. After monitoring the reaction for a short time, we added Axin and observed a sharp increase in the rate of β-catenin phosphorylation (Figure S2.7). These data suggest that formation of the inactive state is reversible. Second, the inactive state is likely a higher-order oligomer, based on kinetic modeling that suggests that the observed rates level off too sharply with increasing GSK3β concentration to fit to a dimer model (Figure 2.4B and Methods).

Taken together, our data suggest a new model for the effect of Axin on the reaction of GSK3β with unprimed β-catenin (Figure S2.8). At low concentrations, GSK3β is predominantly monomeric and active. At high concentrations, the GSK3β•β-catenin complex cooperatively assembles into an inactive, higher-order oligomer. Axin prevents the formation of this higher-order oligomer, which leads to an increase in observed rates for the reaction of GSK3β with β-catenin. The Axin-dependent rate enhancement arises because Axin increases active enzyme concentration, rather than tethering kinase to substrate to directly promote the phosphorylation reaction. Because this effect only occurs for the unprimed β-catenin reaction, and at high GSK3β concentrations, its physiological relevance is uncertain. Cellular GSK3β concentrations estimated from mass spectrometry proteomics datasets[68–70] vary in the range of ~10-300 nM for human HeLa and U2OS cells (cell volumes from BioNumbers BNID 103725 & 108088).[71] These values are similar to the ~100 nM concentration where we see the active/inactive transition *in vitro*, and additional experiments to determine if an oligomeric GSK3β•β-catenin complex exists *in vivo* could be

justified. More importantly, the observation that Axin accelerates the β-catenin reaction *in vitro* was the initial foundation to explain the function of the Wnt pathway destruction complex *in vivo*. We now understand that the mechanistic origin of this effect is quite different than what was originally thought and only applicable in specific conditions.

2.2.4 *Axin slows the GSK3β reaction with CREB, a non-Wnt pathway substrate*

In parallel to experiments with β-catenin, we also assessed whether Axin had any effect on GSK3β reactions with other, non-Wnt pathway substrates. Our initial hypothesis was that Axin would accelerate the β-catenin reaction, but there would be no effect on substrates that do not bind Axin. The experiments described above demonstrate that this hypothesis was incorrect for the β-catenin reaction. As described below, we subsequently found that the hypothesis was also incorrect for non-Wnt pathway substrates, and the unexpected behavior we observed with a non-Wnt pathway substrate provides an alternative model to explain how Axin might control specificity for GSK3β reactions.

To determine how Axin affects reactions with non-Wnt pathway substrates, we measured reaction rates with CREB, a transcription factor that is phosphorylated by GSK3β and integrates signals from a number of pathways.[67,72] PI3K/Akt signaling represses GSK3β activity, which affects CREB-dependent transcription but does not activate Wnt outputs.[54,73] We expected that Axin should have no effect on CREB phosphorylation because Wnt and growth factor signals appear to be insulated from each other *in vivo*,[52–54] and there is no known binding interface for CREB on Axin. Further, the Axin-dependent activation effect that we observed on the β-catenin reaction *in*

vitro arises from Axin interacting with the GSK3β•β-catenin complex, which should not be relevant for the CREB reaction.

We expressed a short CREB peptide ($CREB_{127\text{-}135}$) as an MBP fusion; this peptide is phosphorylated by PKA at Ser133, which serves as a priming site for GSK3β to phosphorylate Ser129 (Figure 2.5A).[74] We phosphorylated $CREB_{127\text{-}135}$ to completion *in vitro* with PKA to produce pS133-$CREB_{127\text{-}135}$ (Figure S2.9). When we measured reaction rates for GSK3β–catalyzed phosphorylation of pS133-$CREB_{127\text{-}135}$, we observed that reaction rates actually decrease substantially in the presence of Axin (Figure 2.5B & C), with the value of k_{cat}/K_M decreasing 35-fold compared to the reaction without Axin (Table 2). The reaction did not detectably saturate in the presence of Axin, suggesting that the K_M has shifted to a larger value and that at least some of the decrease in k_{cat}/K_M arises from a disruption of binding interactions between GSK3β and pS133-$CREB_{127\text{-}135}$. This behavior of Axin was unexpected, as we had initially anticipated that Axin would simply have no effect on the CREB reaction. In hindsight, however, one of the reactions with β-catenin displayed similar behavior. The GSK3β-catalyzed reaction mediated by AxinΔBCD, which does not bind β-catenin, was also significantly slower than the reaction without Axin (Figure S2.5 and S2.6). Together, these results suggest that when Axin does not interact with the GSK3β substrate, either because the substrate does not bind Axin (CREB) or because the substrate binding site on Axin is mutated (AxinΔBCD), Axin actually reduces GSK3β activity. Based on crystal structures, Axin bound to GSK3β does not obviously occlude the active site or the binding site for the phosphoprimed-residue.[56] Thus, the repressive effect of Axin on GSK3β activity may arise from remote, allosteric modulation of the substrate binding surface. This general detrimental effect is mitigated in reactions with β-catenin by binding interactions between Axin

and β-catenin, which results in net effects that are modestly beneficial or neutral for the primed and unprimed β-catenin reactions (Figures 2.2 and 2.3, Table 2).

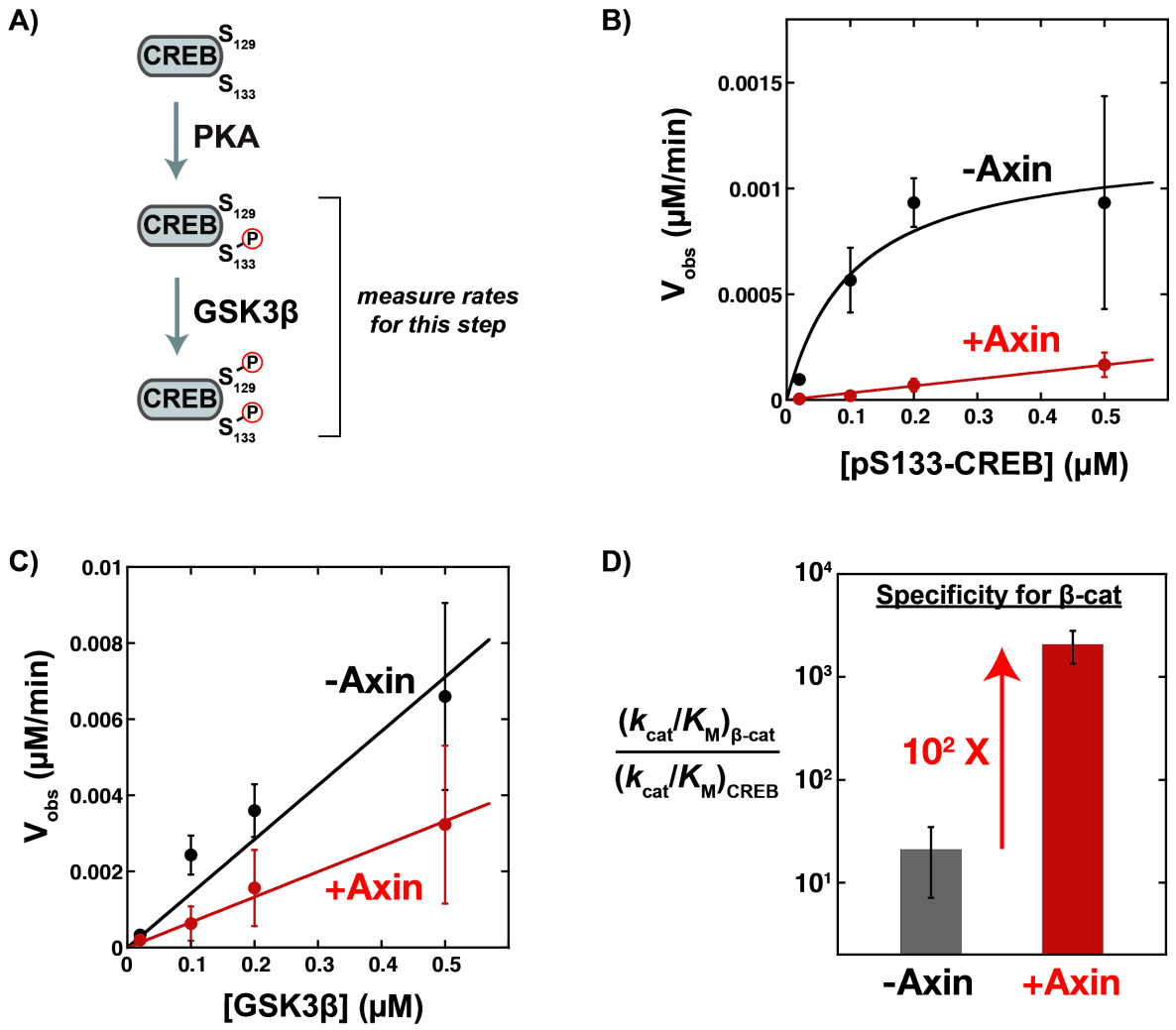

Figure 2.5 Axin significantly decreases the rate of CREB phosphorylation.

(A) Minimal scheme for phosphorylation of CREB. PKA phosphorylates CREB at S133. pS133 serves as a priming site for GSK3β, which phosphorylates pS133-CREB at S129. (B) Michaelis-Menten plot of V_{obs} vs. [pS133-CREB$_{127\text{-}135}$] at 20 nM GSK3β in the presence and absence of 500 nM miniAxin. See Table 2 for values of fitted kinetic parameters. We were unable to detect GSK3β-catalyzed phosphorylation of unprimed CREB ($V_{obs} \leq 3 \times 10^{-5}$ μM/min at 0.5 μM CREB). (C) Plot of V_{obs} vs. [GSK3β] at 500 nM pS133-CREB$_{127\text{-}135}$ in the presence and absence of 500 nM miniAxin. Error bars in (B)-(C) are mean ± SD for at least 3 measurements. (D) The specificity of GSK3β for β-catenin relative to CREB, defined as the ratio of the corresponding k_{cat}/K_M values, increases by 10^2-fold in the presence of Axin.

2.3 Discussion

To understand how Wnt signals regulate Axin to modulate GSK3β activity, we biochemically reconstituted GSK3β-mediated reactions *in vitro* and attempted to reproduce the long-standing result that Axin substantially accelerates the reaction of GSK3β with β-catenin.[56–58] Although prior reports suggested large effects as high as $>10^4$-fold, we found modest 2- to 3-fold effects from Axin on the rate constants for the phosphorylation reaction (Table 2). Two key features of our work can explain this discrepancy. First, we measured *in vitro* reaction rates with the phosphoprimed form of β-catenin, while prior work used unprimed β-catenin. A large Axin-dependent rate enhancement can be observed with unprimed β-catenin, but only in the specific condition of high GSK3β concentration, where Axin prevents the formation of an oligomeric, inactive GSK3β•β-catenin complex (Figure 2.4). No similar inactive state accumulates in the reaction with phosphoprimed β-catenin (Figure 2.2C), which is the preferred substrate of GSK3β *in vivo*. Second, we measured well-defined rate constants in the presence and absence of Axin, while previous reports made indirect comparisons between observed rates, leading to the estimate of a $>10^4$-fold effect from Axin.[56]

Our data lead to a new model suggesting that Axin alone is not sufficient to substantially accelerate the reaction of GSK3β with phosphoprimed β-catenin. This model does not contradict the vast Wnt literature that supports the importance of Axin in Wnt signaling.[28,36,75] Notably, mutations in Axin can have substantial and severe effects on Wnt signaling and vertebrate development.[31,32,76,77] Moreover, the model that the destruction complex acts to accelerate β-catenin phosphorylation is a cornerstone of functional models for Wnt signaling.[30] Thus, while Axin alone may not significantly accelerate β-catenin phosphorylation, other factors not present in our minimal *in vitro*

system may be required to coordinate with Axin and promote the reaction. APC is a particularly intriguing candidate (Figure 2.1B), as it has relatively strong binding sites for β-catenin in the low nM affinity range.[27,63] The Axin-APC complex may be the functional scaffold necessary to promote GSK3β-mediated phosphorylation of β-catenin.[78–80] Post-translational modifications of Axin could also potentially play an important role.[44] Finally, it is possible that the primary mode of regulation of β-catenin phosphorylation could be via controlling the CK1α-mediated phosphopriming step.[27,61] There are conflicting reports on whether Axin accelerates the CK1α-catalyzed reaction *in vitro*,[61,81] and there is evidence that Wnt signals affect both the CK1α and GSK3β-mediated reactions *in vivo*.[59] Our data underscore the importance of quantitative biochemical reconstitution for testing functional models in biology. We now know that molecular-level models that focus on Axin as a scaffold for GSK3β are incomplete, and we can look to other factors that play a role in accelerating β-catenin phosphorylation.

In the absence of a large functional effect from Axin, it remains unclear how GSK3β is independently regulated by different signaling pathways. One possible model is that Axin, together with some as yet unrecognized factor in the destruction complex, significantly accelerates the reaction of GSK3β with β-catenin. A Wnt signal could then disrupt the activity of the destruction complex, which would prevent β-catenin phosphorylation without affecting other substrates of GSK3β. Explaining why growth factor/insulin signals do not cross-activate into Wnt pathway outputs is more challenging. In growth factor/insulin signaling, the kinase Akt phosphorylates GSK3β on Ser9, which autoinhibits GSK3β by occupying the binding pocket for the phosphoprimed residue of the substrate.[66,82] Presumably, blocking the binding pocket for the phosphoprimed residue should also disrupt the reaction with primed β-catenin, since pS45-β-

catenin reacts ~50-fold faster than unprimed β-catenin (Figures 2.2 & 2.3, Table 2), and phosphopriming is necessary for Wnt signaling *in vivo*.[27,61] One possible explanation is that the Wnt-responsive pool of GSK3β is sequestered away from the rest of cellular GSK3β and protected from being phosphorylated by Akt.[54] Consistent with this model, cellular Axin concentrations are substantially lower than GSK3β,[30,68–70,83] which means that there could be an Axin-bound subpopulation and a free, Axin-independent population of GSK3β. Also consistent with this model, we measured the off rate of GSK3β from Axin to be 2.7×10^{-4} s^{-1} (Table 1), which corresponds to a half-time of ~40 minutes. This timescale sets a rough lower limit for how quickly any autoinhibited GSK3β from an Axin-independent pool could exchange on to Axin and crosstalk into Wnt signaling. This off rate is relatively slow for a scaffold-kinase complex and potentially consistent with a sequestration model.[13]

An alternative model to explain how GSK3β is insulated between signaling pathways is suggested by the sharp, 35-fold drop in k_{cat}/K_M towards pS133-CREB in the presence of Axin (Figure 2.5). Together with the modest, 3-fold increase in k_{cat}/K_M towards pS45-β-catenin (Figure 2.2), there is a net 10^2-fold increase in specificity towards β-catenin in the presence of Axin, where specificity is defined by the ratio of the corresponding k_{cat}/K_M values (Figure 2.5D). Thus, GSK3β bound to Axin preferentially reacts with β-catenin, while the Axin-independent pool of GSK3β could be fully saturated with non-Wnt pathway substrates and unable to react with β-catenin. A Wnt signal that disrupts the destruction complex, possibly by releasing GSK3β, would then subject this pool of GSK3β to increased competition from non-Wnt pathway substrates and prevent β-catenin phosphorylation. Because Axin concentrations are low, the amount of GSK3β released into the Axin-independent pool would be small relative to the total amount of GSK3β, and would likely

not significantly perturb phosphorylation rates towards other GSK3β substrates. Insulation of β-catenin from growth factor/insulin signaling would still require additional mechanistic features as described above. While this model is highly speculative, and we lack a clear molecular explanation for how Axin exerts this specificity effect, it has the interesting feature that it does not require Axin to produce a large increase in a rate constant for β-catenin phosphorylation. Instead, Axin accelerates the β-catenin phosphorylation rate by preventing competing substrates from occupying Axin-bound GSK3β.

In addition to the implications for signaling in the Wnt pathway, our results have important implications for our understanding of scaffold proteins in general. Like many scaffold proteins, Axin was originally characterized as a scaffold based on its ability to bind to both a kinase and its substrate.[58] From these binding properties, scaffold proteins are often inferred to exert large increases in kinase reaction rates towards the scaffold-bound substrates. Our results reiterate a critical point, however: binding interactions alone are not sufficient to demonstrate that a scaffold protein enhances kinase activity. Although Axin binds both GSK3β and β-catenin, these binding interactions do not produce substantial increases in the phosphorylation rate. The binding affinity of Axin for β-catenin is relatively weak and may not significantly enhance the ability of GSK3β to interact with β-catenin. Alternatively, Axin alone might simply be too flexible[84] to precisely orient GSK3β and β-catenin in a way that accelerates the reaction. The fact that these issues were overlooked for so long with Axin, an early, prototypical model for scaffold protein behavior, serves as a cautionary reminder that quantitative biochemical studies are critical for assessing the molecular functions of scaffold proteins.

There is an emerging consensus that scaffold proteins can have many functions beyond simply tethering a kinase to its substrate,[5] including allosterically modulating the activity of their target proteins. Our data suggest two important features of the Axin scaffold protein that affect activity and specificity in kinase signaling. First, we observe that Axin can prevent the accumulation of an inactive, oligomeric kinase-substrate complex in the reaction with unprimed β-catenin. Although the *in vivo* relevance of this effect for Wnt signaling is uncertain, it still represents a novel biochemical capability that could play a role in other scaffold-mediated signaling networks. Second, we observe that Axin decreases the activity of GSK3β towards a non-scaffold-dependent substrate, which results in a large specificity switch even without significantly increasing the rate constant for the scaffold-bound substrate. This effect suggests an additional mechanism by which scaffold proteins can encode specificity in cell signaling networks. These insights arose from reconstitution and quantitative kinetic characterization of a minimal biochemical system *in vitro*, which provides a critical framework to evaluate and test functional models for the behavior of biological systems. Future biochemical studies that introduce additional Wnt pathway and GSK3β-interacting proteins will likely provide important new insights and rigorous tests to further expand our understanding of complex, interconnected cell signaling networks.

2.4 Methods and Materials

2.4.1 *Protein Expression Constructs*

The human Wnt pathway proteins GSK3β, β-catenin, and Axin (hAxin1 isoform 2, Uniprot O15169-2) were cloned into *E. coli* expression vectors containing an N-terminal maltose binding protein (MBP) and a C-terminal His6 tag. Human coding sequences were obtained as follows:

GSK3β (addgene #14753)[85], β-catenin (addgene #17198, a gift from Randall Moon), and Axin (derived from hAxin1-rLuc, a gift from Randall Moon). CK1α was cloned with an N-terminal GST tag and a C-terminal His6 tag; the human CK1α sequence was obtained from addgene #92014.[86] The catalytic subunit of mouse PKA was expressed from pET15b with an N-terminal His-tag (addgene #14921).[87] The $CREB_{127-135}$ peptide ILSRRPSYR was cloned by oligo annealing into a vector with an N-terminal MBP and C-terminal His6 tag. The coexpression plasmid for β-catenin and CK1α was constructed by inserting the GST-CK1α expression cassette (without the His6 tag) into the MBP- β-catenin-His plasmid. Axin truncation constructs $Axin_{384-518}$ (miniAxin), $Axin_{\Delta 465-518}$ (AxinΔBCD), and $Axin_{465-518}$ (BCD) were cloned as described for full length Axin above. MiniAxin contains binding sites for both GSK3β and β-catenin. The N-terminal boundary was defined based on the crystal structure of GSK3β with an Axin peptide[56] and the C-terminal boundary was defined based on the Pfam annotation of the BCD (PF08833).[88] The N-terminal boundary of BCD (for AxinΔBCD and BCD) was also defined from the Pfam annotation. A complete list of protein expression constructs is provided in Table 3.

2.4.2 *Protein Expression and Purification*

All Wnt pathway, CREB, and PKA proteins were expressed in Rosetta (DE3) pLysS *E. coli* cells by inducing with 0.5 mM IPTG overnight at 18 ºC. Constructs with N-terminal MBP and C-terminal His6 tags (GSK3β, β-catenin, Axin, and $CREB_{127-135}$) were affinity purified with HisPur Ni-NTA resin (Thermo Scientific) and amylose resin (NEB). CK1α was purified with Ni-NTA resin and glutathione agarose resin (Thermo Scientific). The PKA catalytic subunit was purified on Ni-NTA resin. Purified proteins were dialyzed into 20 mM Tris-HCl pH 8.0, 150 mM NaCl, 10% glycerol, and 2 mM DTT at 4 °C, aliquoted and stored at -80 °C. Protein concentrations were

determined using a Bradford assay (Thermo Scientific). YopH was expressed in BL21 (DE3) *E. coli* cells and purified as previously described.[89]

For quantitative binding assays using bio-layer interferometry, GSK3β was further purified by size exclusion chromatography using a Superdex 200 Increase 10/300 GL column (GE Healthcare) and used immediately.

2.4.3 *Quantitative Western Blotting*

Protein samples were run on 4-15% miniProtean TGX gels (Bio-Rad) and transferred to 0.2 μm nitrocellulose membranes (Bio-rad). Membranes were blocked with 50:50 Li-Cor blocking buffer:TBST, incubated with antibodies as described below using either manual washes or a Precision Biosystems BlotCycler, visualized using the Li-Cor Odyssey Imaging System, and quantified using Image Studio Lite software (Li-Cor).

2.4.4 *Determination of the phosphorylation state of GSK3β*

200 nM purified GSK3β was incubated with 12 μM tyrosine phosphatase (YopH) for 30 minutes in PMP buffer (New England Biolabs) [50 mM HEPES pH 7.5, 100 mM NaCl, 2 mM DTT, 0.01% Brij 35] at 25 ºC. The level of Tyr216 phosphorylation was assessed by western blotting using a primary Anti-GSK-3β (pY216) antibody (BD Biosciences #612312) and a secondary IRDye 800CW Donkey Anti-Mouse IgG antibody (Li-Cor #926-32212). Total GSK3β (MBP-tagged) was detected by western blotting using a primary MBP Tag (8G1) antibody (Cell Signaling Technology #2396) and a secondary IRDye 800CW Donkey Anti-Mouse IgG antibody (Li-Cor #926-32212).

Table 3 Protein expression plasmids.

Plasmid	Protein[a]	Expressed Protein	Vector	Source
pEF019	β-catenin	MBP-β-catenin-His	pMBP-MG[b]	*This study*
pES001	GSK3β	MBP-GSK3β-His	pMBP-MG	*This study*
pEF073	Axin	MBP-Axin-His	pMBP-MG	*This study*
pMG023	$Axin_{384-518}$ (miniAxin)	MBP-$Axin_{384-518}$-His	pMBP-MG	*This study*
pMG035	$Axin_{\Delta 465-518}$ (AxinΔBCD)	MBP-$Axin_{\Delta 465-518}$-His	pMBP-MG	*This study*
pMG022	$Axin_{465-518}$ (BCD)	MBP-$Axin_{465-518}$-His	pMBP-MG	*This study*
pMG046	CK1α	GST-CK1α-His	pETARA	*This study*
pMG051[c]	β-catenin/CK1α	MBP-β-catenin-His/GST-CK1α	pMBP-MG	*This study*
pEF086	CREB (127-135)	MBP-$CREB_{127-135}$-His	pMBP-MG	*This study*
H_6-rC	PKA catalytic subunit	His-PKA-rC	pET15b	Addgene #14921
YopH	YopH	YopH (untagged)	pCDFDuet-1	(Seeliger et al., 2005)

[a] All proteins are human sequences except PKA, which is the mouse sequence.

[b] pMBP-MG is a modified version of pMAL-p2X (New England Biolabs) with an N-terminal TEV-cleavable MBP tag and a C-terminal His6 tag. pETARA contains an N-terminal TEV-cleavable GST tag and a C-terminal His6 tag. pMBP-MG and pETARA were described previously.[14]

[c] pMG051 was constructed by inserting the GST-CK1α expression cassette (without the His tag) from pMG046 into the pEF019 backbone.

2.4.5 *Preparation of phospho-primed β-catenin (pS45-β-catenin)*

For quantitative kinetic and binding assays, pS45-β-catenin was obtained by co-expression with CK1α in *E. coli* and purified as described above for β-catenin.

pS45-β-catenin could also be obtained by *in vitro* phosphorylation of β-catenin with purified CK1α. The phosphorylation reaction was performed in a 5 mL volume with 5 μM β-catenin, 1 μM CK1α, and 500 μM ATP in 40 mM HEPES pH 7.4, 50 mM NaCl, 10 mM $MgCl_2$, 0.05% IGEPAL. The reaction was incubated at 25 ºC for 1.5 hours.

For both co-expressed and *in vitro* phosphorylated pS45-β-catenin, the extent of pS45 phosphorylation was evaluated by western blotting using a primary anti-phospho-β-Catenin

(Ser45) antibody (Cell Signaling Technology #9564) and a secondary IRDye 800CW Goat Anti-Rabbit IgG antibody (Li-Cor #926-32211) (Figure S2.1B).

2.4.6 *Preparation of phosphor-primed CREB (pS133-CREB$_{127-135}$)*

Preparative-scale *in vitro* phosphorylation of CREB$_{127-135}$ at Ser133 was performed in a 10 mL reaction with 13 μM CREB$_{127-135}$, 6.5 μM PKA, and 100 μM ATP in 40 mM HEPES pH 7.4, 50 mM NaCl, 10 mM $MgCl_2$, 0.05% IGEPAL. The reaction was incubated at 25 ºC for 20 minutes. pS133-CREB$_{127-135}$ was purified with amylose resin, concentrated in storage buffer [20 mM Tris-HCl pH 8.0, 150 mM NaCl, 10% glycerol, and 2 mM DTT], aliquoted and stored at -80 °C.

To determine the time necessary for preparative-scale CREB phosphorylation, an analytical-scale phosphorylation reaction was performed with γ-^{32}P-ATP. A 30 μL reaction was conducted with 10 μM CREB$_{127-135}$ and 2 μM PKA in 40 mM HEPES pH 7.4, 50 mM NaCl, 10 mM $MgCl_2$, 0.05% IGEPAL at 25 ºC. The reaction was initiated by adding ATP to a final concentration of 100 μM unlabeled ATP and 0.24 μCi γ-^{32}P-ATP. Timepoints were collected at 5, 10, 20, 40, and 60 minutes. 5 μL aliquots were quenched by spotting on 0.2 μm nitrocellulose membranes (Bio-rad) and placing the membranes in 0.5% v/v phosphoric acid. Membranes were washed 4X 5 min in 0.5% v/v phosphoric acid, allowed to air dry, exposed to a phosphorimager cassette, and imaged on a GE Typhoon FLA 9000. Images were analyzed using ImageQuant 5.1 (GE Healthcare). The data indicated that the reaction approached completion within the first 5-10 minutes (Figure S2.9). We performed preparative scale CREB phosphorylation reactions using a similar concentration of CREB and >3X more PKA, which should go to completion in <20 minutes.

2.4.7 *Quantitative Kinetic Assays*

In vitro kinetic assays were conducted in kinase assay buffer [40 mM HEPES pH 7.4, 50 mM NaCl, 10 mM $MgCl_2$, and 0.05% IGEPAL] at 25 ºC in 60 μL total volume. Reactions were initiated by adding ATP to a final concentration of 100 μM (this concentration of ATP is saturating – see Figure S2.3). Reaction timepoints for initial rate kinetics were obtained at 10, 30, 60, and 90 seconds (pS45-β-catenin reactions); 2, 5, 10, and 20 minutes (unprimed β-catenin reactions); 0.5, 1, 2, and 3 minutes (CREB reactions at [GSK3β] > 20 nM); and 2, 5, 10, and 15 minutes (CREB reactions at [GSK3β] = 20 nM). 10 μL aliquots were quenched by boiling in 5X SDS loading buffer. Samples were analyzed by SDS-PAGE and quantitative western blotting as described above. For reactions with [β-catenin] ≥ 500 nM, gel samples were diluted 2-fold (unprimed β-catenin reactions) or 5-fold (pS45-β-catenin reactions) to prevent a gel smearing artifact.

GSK3β-phosphorylated β-catenin was detected using a primary anti-Phospho-β-Catenin (Ser33/37/Thr41) Antibody (Cell Signaling Technology #9561). GSK3β-phosphorylated CREB was detected using a primary anti-Phospho-CREB (Ser129) Antibody (Thermo Scientific PA5-36843). For both products, the secondary antibody was IRDye 800CW Goat Anti-Rabbit IgG antibody (Li-Cor #926-32211)

Concentrations of phosphorylated β-catenin product were determined by comparing western blot signal intensities to an endpoint standard containing 50 nM β-catenin phosphorylated to completion with GSK3β. The standard was prepared in a reaction with 50 nM β-catenin, 100 nM GSK3β, 100 nM miniAxin, and 100 μM ATP in kinase assay buffer at 25 ºC for 17 hrs.

Concentrations of phosphorylated CREB product were determined similarly with an endpoint standard containing 50 nM CREB phosphorylated to completion with GSK3β. The standard was prepared in a reaction with 50 nM pS133-CREB, 500 nM GSK, 100 μM ATP in kinase assay buffer at 25 ºC for 2.5 hrs.

Kinetic parameters were determined by fitting plots of initial rates (V_{obs}) vs. [substrate] to the Michaelis-Menten equation ($V_{obs} = k_{cat}[E]_0[S]/(K_M+[S])$). In cases where the reaction did not detectably saturate (i.e. the reaction with CREB in the presence of Axin), the value of k_{cat}/K_M was obtained from the slope of a linear fit to a plot of V_{obs} vs. [substrate]. For the inactive GSK3β oligomer model (Figure 2.4), the data were fit to the equation: $[GSK3\beta]_{total} = (V_{obs}/k_{cat}) + (N/K_{oligomer})\times(V_{obs}/k_{cat})^N$.

2.4.8 *Quantitative Binding Assays*

Binding affinities (K_D) and the corresponding association and dissociation rate constants (k_a and k_d) were determined using bio-layer interferometry using an Octet Red96e system (ForteBio) with Streptavidin biosensor tips. Proteins were biotinylated using an EZ-Link Micro NHS-PEG4-Biotinylation kit (Thermo Scientific) with a molar coupling ratio of 1:1 and purified using 7K MWCO Zeba Spin Desalting Columns (Thermo Scientific). Binding assays were performed in 10 mM Na_2HPO_4/NaH_2PO_4 pH 7.4, 137 mM NaCl, 2.6 mM KCl, 0.1% BSA, and 0.02% Tween-20 at 22 °C with Greiner Bio-One 96-Well Non-treated Polypropylene Microplates (Fisher Scientific) at a shake speed of 1000 rpm. Well volumes were 200 μL. Background buffer effects were corrected using a buffer reference sample (a tip loaded with biotinylated protein and dipped into buffer instead of analyte). The buffer reference sample was subtracted from the binding assay data

before analysis. Data were analyzed using Data Analysis HT 11.0 (ForteBio) to obtain values of K_D, k_a and k_d.

For the binding interaction between GSK3β and miniAxin, the miniAxin protein was biotinylated. Biosensor tips were hydrated for 10 minutes in assay buffer, equilibrated for 1 minute, and then loaded with 10 nM biotinylated miniAxin for 5 minutes. After a 1 minute equilibration in assay buffer, tips were immersed in varying concentrations of GSK3β (500 nM, 250 nM, 125 nM, 62.5 nM, 31.3 nM, 15.6 nM, and 7.81 nM) for 5 minutes to monitor association kinetics. Tips were then immersed in assay buffer for 10 minutes to measure dissociation kinetics.

For the binding interaction between pS45-β-catenin and miniAxin, pS45-β-catenin was biotinylated. Biosensor tips were hydrated for 10 minutes in assay buffer, equilibrated for 1 minute, and then loaded with 30 nM nM biotinylated pS45-β-catenin for 5 minutes. After a 1 minute equilibration in assay buffer, tips were immersed in varying concentrations of miniAxin (20 μM, 10 μM, 5 μM, 2.5 μM, 1.25 μM, 625 nM, 312.5 nM) for 5 minutes to monitor association kinetics. Tips were then immersed in assay buffer for 10 minutes to measure dissociation kinetics.

2.5 Supplemental Figures

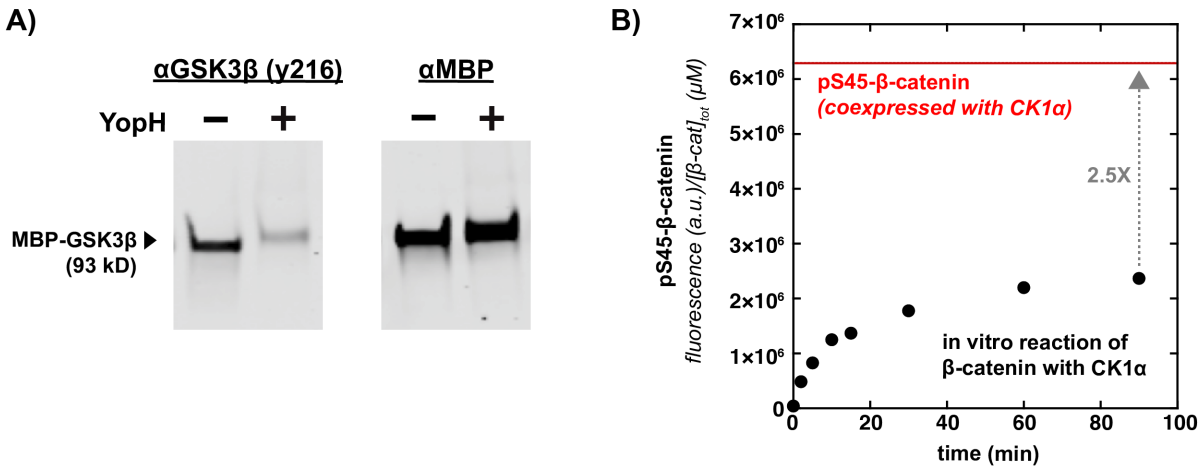

Figure S2. 1 GSK3β purification

(A) GSK3β purified from *E. coli* is phosphorylated on the activation loop Tyr216. Purified GSK3β was incubated with the tyrosine phosphatase YopH and analyzed by western blot using an antibody specific for pY216 GSK3β. Purified GSK3β produced a detectable signal at the expected molecular weight (94 kD), and the signal decreases substantially upon YopH treatment. The loading control indicates no change in total GSK3β (using an anti-MBP antibody that detects the MBP tag on purified GSK3β). (B) β-catenin co-expressed with CK1α in *E. coli* is phosphorylated on Ser45. The extent of S45 phosphorylation was detected by western blot using an antibody specific for pS45-β-catenin. Phosphoprimed β-catenin can also be obtained by incubating β-catenin with purified CK1α. In this reaction, we observe partial phosphorylation of Ser45, with a total pS45 signal (normalized to total protein concentration) reaching only ~40% of that obtained when β-catenin is co-expressed with CK1α.

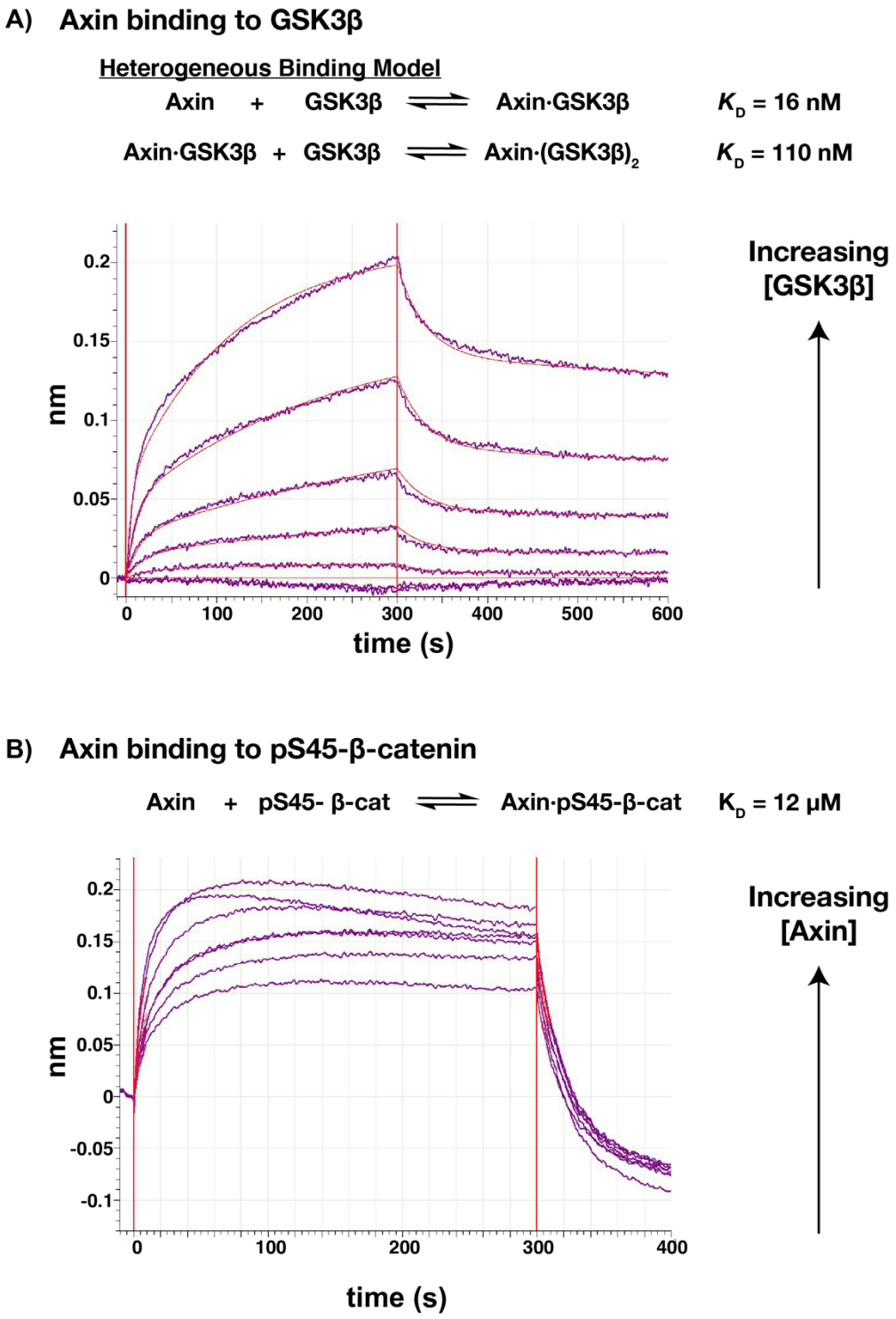

Figure S2. 2 Axin binding to GSK3β and β-catenin.

(A) Bio-layer interferometry traces showing association and dissociation of GSK3β to immobilized biotinylated miniAxin. The data were fit to a Heterogeneous Binding Model (Data Analysis HT 11.0, ForteBio) that accounts for GSK3β binding to Axin and GSK3β dimerization.[42] This fit gives a K_D of 16

nM for Axin binding to GSK3β and a K_D of 110 nM for GSK3β dimerization. A 1:1 binding model that neglects GSK3β dimerization gives a poor fit to the data. The interferometry traces for GSK3β binding to biotinylated full length Axin and AxinΔBCD (Figure S2.4) were similar. Values of fitted binding constants are reported in Table 1. (B) Bio-layer interferometry traces showing association and dissociation of miniAxin to immobilized biotinylated pS45-β-catenin. This binding event produced a negative shift in the interferometry signal (the data are displayed with an inverted y-axis), indicating a compression in the surface which could indicate a major conformational change in the bound complex. The data were fit using a 1:1 binding model for the first 10 seconds each of the association and dissociation phases, as there was a significant baseline drift even after background correction (see Methods) that caused significant errors if the full timecourse was included in the fit.

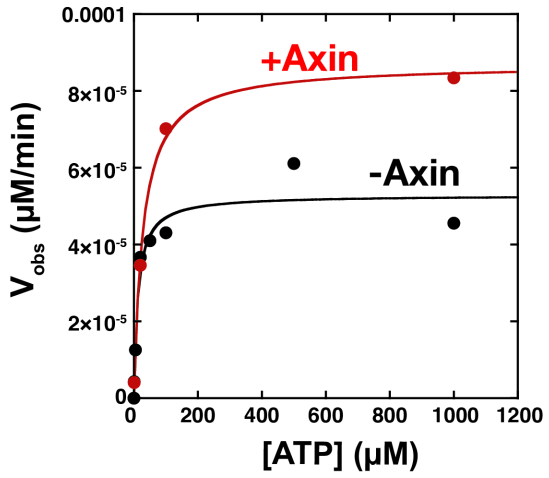

Figure S2. 3 The concentration of ATP is saturating

The concentration of ATP used for quantitative kinetic experiments (100 μM) is saturating in the presence and absence of Axin. Michaelis-Menten plot of V_{obs} vs. [ATP] at 20 nM GSK3β and 500 nM β-catenin in the presence and absence of 100 nM miniAxin. Fits to the Michaelis-Menten equation give $K_{M,\,ATP}$ values of 12 ± 4 μM and 28 ± 3 μM in the presence and absence of Axin, respectively.

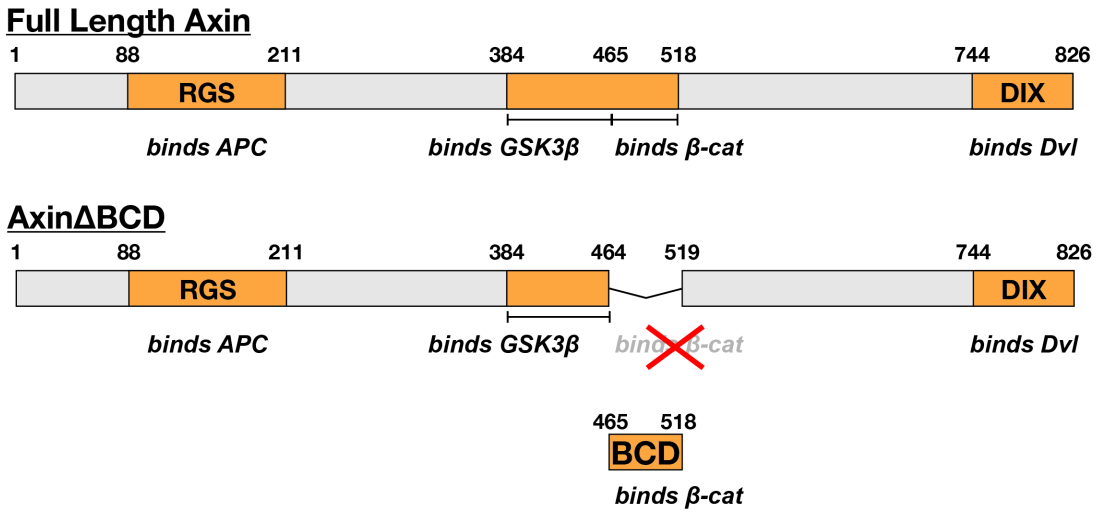

Figure S2. 4 Schematics of Axin fragments
Schematics of full length Axin, AxinΔBCD, and the BCD (see Methods for explanation of domain boundaries).

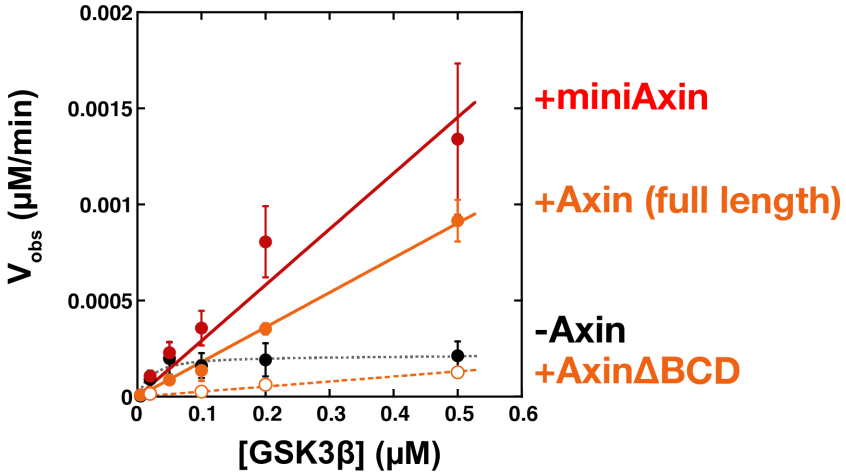

Figure S2. 5 Vary GSK3β in the presence and absence of AxinΔBCD

Plots of V_{obs} vs. [GSK3β] at 500 nM β-catenin in the presence and absence of 500 nM Axin (either miniAxin, full length Axin, or AxinΔBCD). Error bars are mean ± SD for at least 3 measurements.

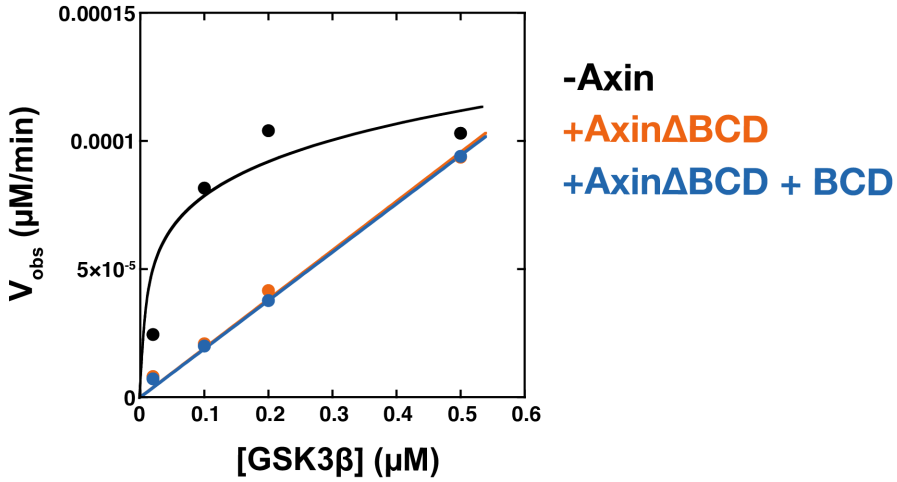

Figure S2. 6 Vary GSK3β in the presence and absence of AxinΔBCD and BCD

Plot of V_{obs} vs. [GSK3β] at 500 nM β-catenin in the presence and absence of 500 nM AxinΔBCD or 500 nM each AxinΔBCD and BCD. In the absence of Axin, the data are fit to a kinetic model with an inactive oligomer state (N=5) as in Figure 2.4B.

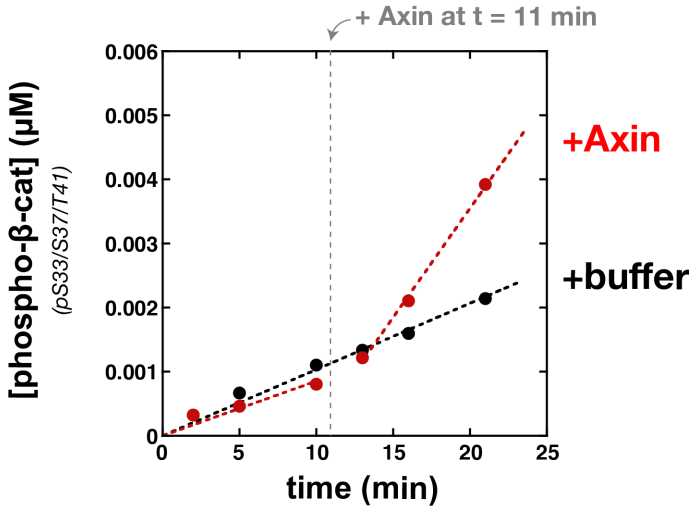

Figure S2. 7 The inactive state of GSK3β is reversible

Product vs. time plot for a reaction with 500 nM GSK3β and 500 nM β-catenin. At t = 11 min, miniAxin was added to a final concentration of 500 nM and the reaction rate sharply increases. A control reaction in which an equal volume of buffer was added shows no change in rate.

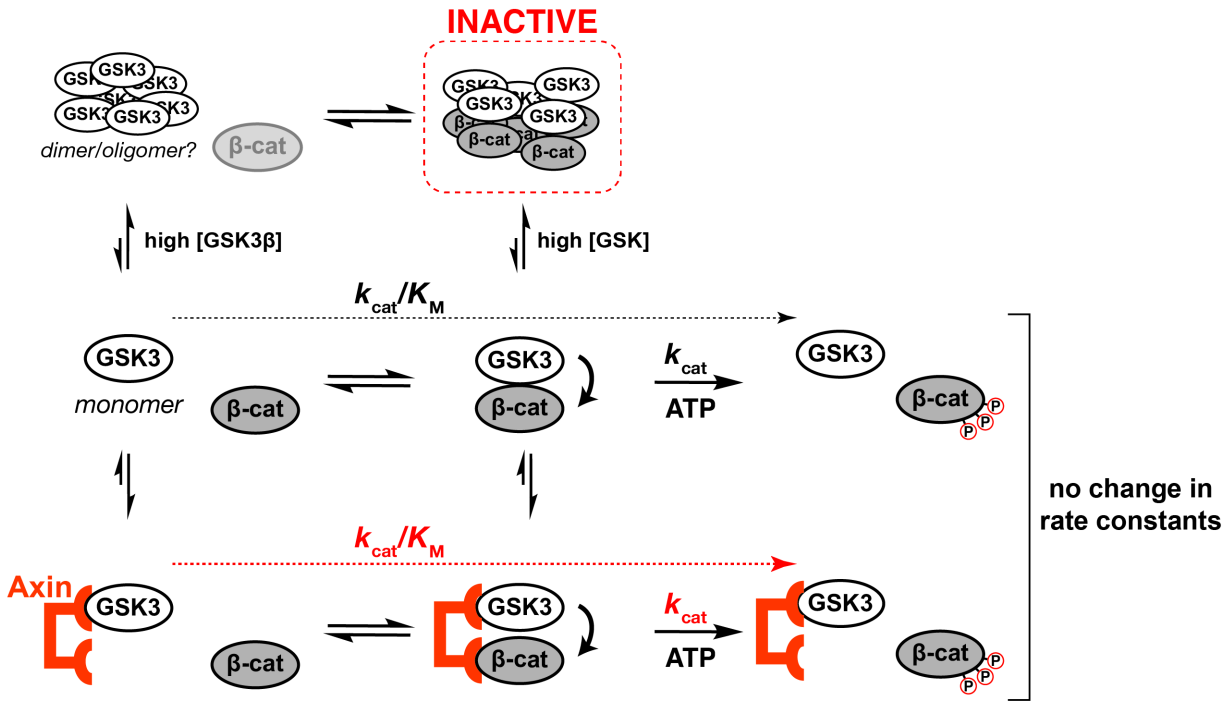

Figure S2. 8 Kinetic model for unprimed β-catenin

A revised kinetic model for the effect of Axin on the reaction of GSK3β with unprimed β-catenin. At low [GSK3β], Axin has no significant effect on the steady state rate constants for the reaction (Figure 2.3B). At high [GSK3β], an oligomeric, inactive complex of GSK3β•β-catenin can accumulate. Axin prevents the formation of this inactive complex. For completeness, the scheme shows a dimer or oligomer of free GSK3β in the absence of β-catenin, as there is evidence that free GSK3β can dimerize (Figure S2.2), but based on the kinetic data the kinetically significant inactive state is the oligomeric GSK3β•β-catenin complex.

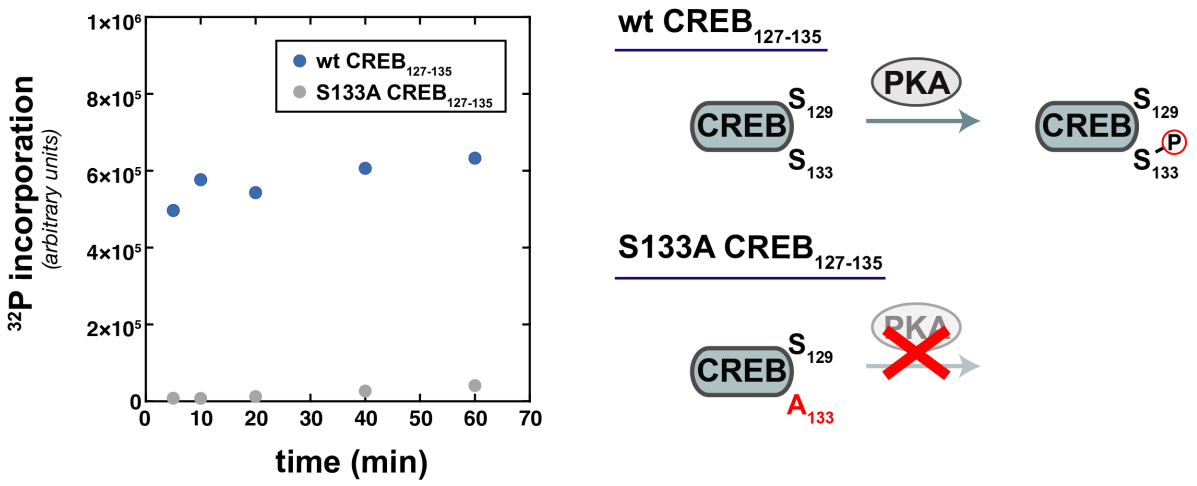

Figure S2. 9 PKA priming of CREB

PKA phosphorylates $CREB_{127\text{-}135}$ on Ser_{133}. Reactions were performed with 10 μM $CREB_{127\text{-}135}$, 2 μM PKA, 100 μM ATP, and trace γ-^{32}P-ATP as described in the Methods section. ^{32}P incorporation into $CREB_{127\text{-}135}$ rapidly approaches completion within the first 5-10 minutes of the reaction. No significant ^{32}P incorporation is detectable in S133A $CREB_{127\text{-}135}$, which indicates that wt $CREB_{127\text{-}135}$ is phosphorylated on Ser_{133}.

BIBLIOGRAPHY

1. Bhattacharyya, R. P., Reményi, A., Yeh, B. J. & Lim, W. A. Domains, Motifs, and Scaffolds: The Role of Modular Interactions in the Evolution and Wiring of Cell Signaling Circuits. *Annu. Rev. Biochem.* **75**, 655–680 (2006).
2. Weng, G. Complexity in Biological Signaling Systems. *Science* **284**, 92–96 (1999).
3. Gordon, M. D. & Nusse, R. Wnt Signaling: Multiple Pathways, Multiple Receptors, and Multiple Transcription Factors. *J. Biol. Chem.* **281**, 22429–22433 (2006).
4. McNeill, H. & Woodgett, J. R. When pathways collide: collaboration and connivance among signaling proteins in development. *Nat. Rev. Mol. Cell Biol.* **11**, 404–413 (2010).
5. Good, M. C., Zalatan, J. G. & Lim, W. A. Scaffold Proteins: Hubs for Controlling the Flow of Cellular Information. *Science* **332**, 680–686 (2011).
6. Luo, W. & Lin, S.-C. Axin: A Master Scaffold for Multiple Signaling Pathways. *Neurosignals* **13**, 99–113 (2004).
7. Liu, W. *et al.* The INAD Scaffold Is a Dynamic, Redox-Regulated Modulator of Signaling in the Drosophila Eye. *Cell* **145**, 1088–1101 (2011).
8. Tsunoda, S. & Zuker, C. S. The organization of INAD-signaling complexes by a multivalent PDZ domain protein in Drosophila photoreceptor cells ensures sensitivity and speed of signaling. *Cell Calcium* **26**, 165–171 (1999).
9. Tsunoda, S. *et al.* A multivalent PDZ-domain protein assembles signaling complexes in a G-protein-coupled cascade. *Nature* **388**, 243–249 (1997).
10. Smith, F. D. *et al.* Local protein kinase A action proceeds through intact holoenzymes. *Science* **356**, 1288–1293 (2017).
11. Langeberg, L. K. & Scott, J. D. Signalling scaffolds and local organization of cellular behaviour. *Nat. Rev. Mol. Cell Biol.* **16**, 232–244 (2015).
12. Burack, W. R. & Shaw, A. S. Signal transduction: hanging on a scaffold. *Curr. Opin. Cell Biol.* **12**, 211–216 (2000).

13. Zalatan, J. G., Coyle, S. M., Rajan, S., Sidhu, S. S. & Lim, W. A. Conformational Control of the Ste5 Scaffold Protein Insulates Against MAP Kinase Misactivation. *Science* **337**, 1218–1222 (2012).

14. Good, M., Tang, G., Singleton, J., Reményi, A. & Lim, W. A. The Ste5 Scaffold Directs Mating Signaling by Catalytically Unlocking the Fus3 MAP Kinase for Activation. *Cell* **136**, 1085–1097 (2009).

15. Morrison, D. K. KSR: a MAPK scaffold of the Ras pathway? *J. Cell Sci.* **114**, 1609–1612 (2001).

16. Nguyen, A. *et al.* Kinase Suppressor of Ras (KSR) Is a Scaffold Which Facilitates Mitogen-Activated Protein Kinase Activation In Vivo. *Mol. Cell. Biol.* **22**, 3035–3045 (2002).

17. McKay, M. M., Ritt, D. A. & Morrison, D. K. Signaling dynamics of the KSR1 scaffold complex. *Proc. Natl. Acad. Sci.* **106**, 11022–11027 (2009).

18. Whitmarsh, A. J. A Mammalian Scaffold Complex That Selectively Mediates MAP Kinase Activation. *Science* **281**, 1671–1674 (1998).

19. Willoughby, E. A., Perkins, G. R., Collins, M. K. & Whitmarsh, A. J. The JNK-interacting Protein-1 Scaffold Protein Targets MAPK Phosphatase-7 to Dephosphorylate JNK. *J. Biol. Chem.* **278**, 10731–10736 (2003).

20. Dodge, K. L. mAKAP assembles a protein kinase A/PDE4 phosphodiesterase cAMP signaling module. *EMBO J.* **20**, 1921–1930 (2001).

21. Mccahill, A. *et al.* In resting COS1 cells a dominant negative approach shows that specific, anchored PDE4 cAMP phosphodiesterase isoforms gate the activation, by basal cyclic AMP production, of AKAP-tethered protein kinase A type II located in the centrosomal region. *Cell. Signal.* **17**, 1158–1173 (2005).

22. Lin, J. & Weiss, A. Identification of the Minimal Tyrosine Residues Required for Linker for Activation of T Cell Function. *J. Biol. Chem.* **276**, 29588–29595 (2001).

23. Strickfaden, S. C. *et al.* A Mechanism for Cell-Cycle Regulation of MAP Kinase Signaling in a Yeast Differentiation Pathway. *Cell* **128**, 519–531 (2007).

24. Yost, C. *et al.* The axis-inducing activity, stability, and subcellular distribution of β catenin is regulated in Xenopus embryos by glycogen synthase kinase 3. *Genes Dev.* **10**, 1443–1454 (1996).

25. Peifer, M., Pai, L.-M. & Casey, M. Phosphorylation of the Drosophila Adherens Junction Protein Armadillo: Roles for Wingless Signal and Zeste-white 3 Kinase. *Dev. Biol.* **166**, 543–556 (1994).

26. Kikuchi, A. Regulation of β-Catenin Signaling in the Wnt Pathway. *Biochem. Biophys. Res. Commun.* **268**, 243–248 (2000).

27. Liu, C. *et al.* Control of β-Catenin Phosphorylation/Degradation by a Dual-Kinase Mechanism. *Cell* **108**, 837–847 (2002).

28. Nusse, R. & Clevers, H. Wnt/β-Catenin Signaling, Disease, and Emerging Therapeutic Modalities. *Cell* **169**, 985–999 (2017).

29. Salic, A., Lee, E., Mayer, L. & Kirschner, M. W. Control of β-Catenin Stability. *Mol. Cell* **5**, 523–532 (2000).

30. Lee, E., Salic, A., Krüger, R., Heinrich, R. & Kirschner, M. W. The Roles of APC and Axin Derived from Experimental and Theoretical Analysis of the Wnt Pathway. *PLoS Biol.* **1**, e10 (2003).

31. Zeng, L. *et al.* The Mouse Fused Locus Encodes Axin, an Inhibitor of the Wnt Signaling Pathway That Regulates Embryonic Axis Formation. *Cell* **90**, 181–192 (1997).

32. Satoh, S. *et al.* AXIN1 mutations in hepatocellular carcinomas, and growth suppression in cancer cells by virus-mediated transfer of AXIN1. *Nat. Genet.* **24**, 245–250 (2000).

33. Mi, K., Dolan, P. J. & Johnson, G. V. W. The Low Density Lipoprotein Receptor-related Protein 6 Interacts with Glycogen Synthase Kinase 3 and Attenuates Activity. *J. Biol. Chem.* **281**, 4787–4794 (2006).

34. Cselenyi, C. S. *et al.* LRP6 transduces a canonical Wnt signal independently of Axin degradation by inhibiting GSK3's phosphorylation of β-catenin. *Proc. Natl. Acad. Sci.* **105**, 8032–8037 (2008).

35. Tortelote, G. G., Reis, R. R., de Almeida Mendes, F. & Abreu, J. G. Complexity of the Wnt/β-catenin pathway: Searching for an activation model. *Cell. Signal.* **40**, 30–43 (2017).

36. MacDonald, B. T., Tamai, K. & He, X. Wnt/β-Catenin Signaling: Components, Mechanisms, and Diseases. *Dev. Cell* **17**, 9–26 (2009).

37. Taelman, V. F. *et al.* Wnt Signaling Requires Sequestration of Glycogen Synthase Kinase 3 inside Multivesicular Endosomes. *Cell* **143**, 1136–1148 (2010).

38. Liu, X., Rubin, J. S. & Kimmel, A. R. Rapid, Wnt-Induced Changes in GSK3β Associations that Regulate β-Catenin Stabilization Are Mediated by Gα Proteins. *Curr. Biol.* **15**, 1989–1997 (2005).

39. Logan, C. Y. & Nusse, R. The Wnt Signaling Pathway in Development and Disease. *Annu. Rev. Cell Dev. Biol.* **20**, 781–810 (2004).

40. Malbon, C. C. & Wang, H. Dishevelled: A Mobile Scaffold Catalyzing Development. in *Current Topics in Developmental Biology* **72**, 153–166 (Elsevier, 2005).

41. Thomas, G. M. *et al.* A GSK3-binding peptide from FRAT1 selectively inhibits the GSK3-catalysed phosphorylation of Axin and β-catenin. *FEBS Lett.* **458**, 247–251 (1999).

42. Fraser, E. *et al.* Identification of the Axin and Frat Binding Region of Glycogen Synthase Kinase-3. *J. Biol. Chem.* **277**, 2176–2185 (2002).

43. Li, L. Axin and Frat1 interact with Dvl and GSK, bridging Dvl to GSK in Wnt-mediated regulation of LEF-1. *EMBO J.* **18**, 4233–4240 (1999).

44. Kim, S.-E. *et al.* Wnt Stabilization of β-Catenin Reveals Principles for Morphogen Receptor-Scaffold Assemblies. *Science* **340**, 867–870 (2013).

45. Jiang, Y., Luo, W. & Howe, P. H. Dab2 stabilizes Axin and attenuates Wnt/β-catenin signaling by preventing protein phosphatase 1 (PP1)–Axin interactions. *Oncogene* **28**, 2999–3007 (2009).

46. Wodarz, A. & Nusse, R. Mechanisms of Wnt Signaling in Development. *Annu. Rev. Cell Dev. Biol.* **14**, 59–88 (1998).

47. Xu, Z. *et al.* Wnt/β-catenin signaling promotes self-renewal and inhibits the primed state transition in naïve human embryonic stem cells. *Proc. Natl. Acad. Sci.* 201613849 (2016). doi:10.1073/pnas.1613849113

48. Polakis, P. The adenomatous polyposis coli (APC) tumor suppressor. *Biochim. Biophys. Acta BBA - Rev. Cancer* **1332**, F127–F147 (1997).

49. Polakis, P. The oncogenic activation of β-catenin. *Curr. Opin. Genet. Dev.* **9**, 15–21 (1999).

50. Madan, B. *et al.* Bone loss from Wnt inhibition mitigated by concurrent alendronate therapy. *Bone Res.* **6**, 17 (2018).

51. Kaidanovich-Beilin, O. & Woodgett, J. R. GSK-3: Functional Insights from Cell Biology and Animal Models. *Front. Mol. Neurosci.* **4**, (2011).

52. Ding, V. W., Chen, R.-H. & McCormick, F. Differential Regulation of Glycogen Synthase Kinase 3β by Insulin and Wnt Signaling. *J. Biol. Chem.* **275**, 32475–32481 (2000).

53. McManus, E. J. *et al.* Role that phosphorylation of GSK3 plays in insulin and Wnt signaling defined by knockin analysis. *EMBO J.* **24**, 1571–1583 (2005).

54. Ng, S. S. *et al.* Phosphatidylinositol 3-Kinase Signaling Does Not Activate the Wnt Cascade. *J. Biol. Chem.* **284**, 35308–35313 (2009).

55. Park, S.-H. Rewiring MAP Kinase Pathways Using Alternative Scaffold Assembly Mechanisms. *Science* **299**, 1061–1064 (2003).

56. Dajani, R. Structural basis for recruitment of glycogen synthase kinase 3beta to the axin-APC scaffold complex. *EMBO J.* **22**, 494–501 (2003).

57. Hart, M. J., de los Santos, R., Albert, I. N., Rubinfeld, B. & Polakis, P. Downregulation of β-catenin by human Axin and its association with the APC tumor suppressor, β-catenin and GSK3β. *Curr. Biol.* **8**, 573–581 (1998).

58. Ikeda, S. Axin, a negative regulator of the Wnt signaling pathway, forms a complex with GSK-3beta and beta -catenin and promotes GSK-3beta -dependent phosphorylation of beta -catenin. *EMBO J.* **17**, 1371–1384 (1998).

59. Hernandez, A. R., Klein, A. M. & Kirschner, M. W. Kinetic Responses of β-Catenin Specify the Sites of Wnt Control. *Science* **338**, 1337–1340 (2012).

60. Li, V. S. W. *et al.* Wnt Signaling through Inhibition of β-Catenin Degradation in an Intact Axin1 Complex. *Cell* **149**, 1245–1256 (2012).

61. Amit, S. Axin-mediated CKI phosphorylation of beta -catenin at Ser 45: a molecular switch for the Wnt pathway. *Genes Dev.* **16**, 1066–1076 (2002).

62. Wang, Q. M., Fiol, C. J., DePaoli-Roach, A. A. & Roach, P. J. Glycogen synthase kinase-3 beta is a dual specificity kinase differentially regulated by tyrosine and serine/threonine phosphorylation. *J. Biol. Chem.* **269**, 14566–14574 (1994).

63. Xing, Y. Crystal structure of a β-catenin/Axin complex suggests a mechanism for the β-catenin destruction complex. *Genes Dev.* **17**, 2753–2764 (2003).

64. Choi, H.-J., Huber, A. H. & Weis, W. I. Thermodynamics of beta-Catenin-Ligand Interactions: The Roles of the N- and C-terminal Tails in Modulating Binding Affinity. *J. Biol. Chem.* **281**, 1027–1038 (2006).

65. Levchenko, A., Bruck, J. & Sternberg, P. W. Scaffold proteins may biphasically affect the levels of mitogen-activated protein kinase signaling and reduce its threshold properties. *Proc. Natl. Acad. Sci.* **97**, 5818–5823 (2000).

66. Frame, S., Cohen, P. & Biondi, R. M. A Common Phosphate Binding Site Explains the Unique Substrate Specificity of GSK3 and Its Inactivation by Phosphorylation. *Mol. Cell* **7**, 1321–1327 (2001).

67. Fiol, C. J. *et al.* A secondary phosphorylation of CREB341 at Ser129 is required for the cAMP-mediated control of gene expression. A role for glycogen synthase kinase-3 in the control of gene expression. *J. Biol. Chem.* **269**, 32187–32193 (1994).

68. Beck, M. *et al.* The quantitative proteome of a human cell line. *Mol. Syst. Biol.* **7**, 549–549 (2014).

69. Itzhak, D. N., Tyanova, S., Cox, J. & Borner, G. H. Global, quantitative and dynamic mapping of protein subcellular localization. *eLife* **5**, (2016).

70. Nagaraj, N. *et al.* Deep proteome and transcriptome mapping of a human cancer cell line. *Mol. Syst. Biol.* **7**, 548–548 (2014).

71. Milo, R., Jorgensen, P., Moran, U., Weber, G. & Springer, M. BioNumbers—the database of key numbers in molecular and cell biology. *Nucleic Acids Res.* **38**, D750–D753 (2010).

72. Shaywitz, A. J. & Greenberg, M. E. CREB: A Stimulus-Induced Transcription Factor Activated by A Diverse Array of Extracellular Signals. *Annu. Rev. Biochem.* **68**, 821–861 (1999).

73. Tullai, J. W. *et al.* Glycogen Synthase Kinase-3 Represses Cyclic AMP Response Element-binding Protein (CREB)-targeted Immediate Early Genes in Quiescent Cells. *J. Biol. Chem.* **282**, 9482–9491 (2007).

74. Fiol, C. J. *et al.* A secondary phosphorylation of CREB341 at Ser129 is required for the cAMP-mediated control of gene expression. A role for glycogen synthase kinase-3 in the control of gene expression. *J. Biol. Chem.* **269**, 32187–32193 (1994).

75. Stamos, J. L. & Weis, W. I. The β-Catenin Destruction Complex. *Cold Spring Harb. Perspect. Biol.* **5**, a007898–a007898 (2013).

76. Anvarian, Z. *et al.* Axin cancer mutants form nanoaggregates to rewire the Wnt signaling network. *Nat. Struct. Mol. Biol.* **23**, 324–332 (2016).

77. Peterson-Nedry, W. *et al.* Unexpectedly robust assembly of the Axin destruction complex regulates Wnt/Wg signaling in Drosophila as revealed by analysis in vivo. *Dev. Biol.* **320**, 226–241 (2008).

78. Hinoi, T. *et al.* Complex Formation of Adenomatous Polyposis Coli Gene Product and Axin Facilitates Glycogen Synthase Kinase-3β-dependent Phosphorylation of β-Catenin and Down-regulates β-Catenin. *J. Biol. Chem.* **275**, 34399–34406 (2000).

79. Ji, L. *et al.* Identification of ICAT as an APC Inhibitor, Revealing Wnt-Dependent Inhibition of APC-Axin Interaction. *Mol. Cell* **72**, 37-47.e4 (2018).

80. Kishida, S. *et al.* Axin, a Negative Regulator of the Wnt Signaling Pathway, Directly Interacts with Adenomatous Polyposis Coli and Regulates the Stabilization of β-Catenin. *J. Biol. Chem.* **273**, 10823–10826 (1998).

81. Sobrado, P., Jedlicki, A., Bustos, V. H., Allende, C. C. & Allende, J. E. Basic region of residues 228-231 of protein kinase CK1 is involved in its interaction with axin: Binding to axin does not affect the kinase activity. *J. Cell. Biochem.* **94**, 217–224 (2005).

82. Cross, D. A. E., Alessi, D. R., Cohen, P., Andjelkovich, M. & Hemmings, B. A. Inhibition of glycogen synthase kinase-3 by insulin mediated by protein kinase B. *Nature* **378**, 785–789 (1995).

83. Geiger, T., Wehner, A., Schaab, C., Cox, J. & Mann, M. Comparative Proteomic Analysis of Eleven Common Cell Lines Reveals Ubiquitous but Varying Expression of Most Proteins. *Mol. Cell. Proteomics* **11**, M111.014050 (2012).

84. Noutsou, M. *et al.* Critical Scaffolding Regions of the Tumor Suppressor Axin1 Are Natively Unfolded. *J. Mol. Biol.* **405**, 773–786 (2011).

85. He, X., Saint-Jeannet, J.-P., Woodgett, J. R., Varmus, H. E. & Dawid, I. B. Glycogen synthase kinase-3 and dorsoventral patterning in Xenopus embryos. *Nature* **374**, 617–622 (1995).

86. Golden, R. J. *et al.* An Argonaute phosphorylation cycle promotes microRNA-mediated silencing. *Nature* **542**, 197–202 (2017).

87. Narayana, N., Cox, S., Shaltiel, S., Taylor, S. S. & Xuong, N. Crystal structure of a polyhistidine-tagged recombinant catalytic subunit of cAMP-dependent protein kinase complexed with the peptide inhibitor PKI(5-24) and adenosine. *Biochemistry* **36**, 4438–4448 (1997).

88. El-Gebali, S. *et al.* The Pfam protein families database in 2019. *Nucleic Acids Res.* **47**, D427–D432 (2019).

89. Seeliger, M. A. *et al.* High yield bacterial expression of active c-Abl and c-Src tyrosine kinases. *Protein Sci.* **14**, 3135–3139 (2005).